Late Cenozoic reorganization of the Arabia-Eurasia collision and the comparison of short-term and long-term deformation rates

Mark Allen

CASP, Department of Earth Sciences, University of Cambridge, Cambridge, UK

James Jackson and Richard Walker

Bullard Laboratories, Department of Earth Sciences, University of Cambridge, Cambridge, UK

Received 31 March 2003; revised 28 November 2003; accepted 16 January 2004; published 17 March 2004.

[1] The Arabia-Eurasia collision deforms an area of ~3,000,000 km^2 of continental crust, making it one of the largest regions of convergent deformation on Earth. There are now estimates for the active slip rates, total convergence and timing of collision-related deformation of regions from western Turkey to eastern Iran. This paper shows that extrapolating the present day slip rates of many active fault systems for ~3–7 million years accounts for their total displacement. This result means that the present kinematics of the Arabia-Eurasia collision are unlikely be the same as at its start, which was probably in the early Miocene (16–23 Ma) or earlier. In some, but not all, active fault systems, short-term (~10 year) and long-term (~5 million year) average deformation rates are consistent. There is little active thickening across the Turkish-Iranian plateau and, possibly, the interior of the Greater Caucasus. These are two areas where present shortening rates would need more than 7 million years to account for the total crustal thickening, and where there are structural and/or stratigraphic data for pre-late Miocene deformation. We suggest that once thick crust (up to 60 km) built up in the Turkish-Iranian plateau and the Greater Caucasus, convergence took place more easily by crustal shortening in less elevated regions, such as the Zagros Simple Folded Zone, the South Caspian region and foothills of the Greater Caucasus, or in other ways, such as westward transport of Turkey between the North and East Anatolian faults. The time and duration of this changeover are not known for certain and are likely be diachronous, although deformation started or intensified in many of the currently active fault systems at ~5 ± 2 Ma. *INDEX TERMS:* 8102 Tectonophysics: Continental contractional orogenic belts; 8158 Tectonophysics: Plate motions—present and recent (3040); 9320 Information Related to Geographic Region: Asia; *KEYWORDS:* collision, Arabia, Eurasia. **Citation:** Allen, M., J. Jackson, and R. Walker (2004), Late Cenozoic reorganization of the Arabia-Eurasia collision and the comparison of short-term and long-term deformation rates, *Tectonics*, *23*, TC2008, doi:10.1029/2003TC001530.

0278-7407/04/2003TC001530$12.00

1. Introduction and Tectonic Setting

[2] This paper summarizes active slip rates, total strain and the timing of collision-related deformation from western Turkey to eastern Iran, based on GPS data, seismicity, and geologic data for total fault displacements and the timing of the onset of deformation. It shows that if present day slip rates are extrapolated for 3–7 million years they account for the total shortening or strike-slip offset on many active fault systems of the Arabia-Eurasia collision zone. We examine the implications of this result, given that initial collision took place as long ago as the early Miocene (~16–23 Ma) [*Robertson*, 2000], in particular how plate convergence might have occurred in different regions over this time. This is relevant to the long-term evolution of continental collisions in general. It is also relevant to the idea that the Arabia-Eurasia collision underwent a reorganization at about 5 Ma, previously suggested for this time because of the initiation or acceleration of strain in fold and fault systems, rapid exhumation of mountain belts and rapid subsidence in adjacent basins [*Wells*, 1969; *Westaway*, 1994; *Axen et al.*, 2001]. We examine possible explanations for this reorganization, which include: opening of the Red Sea; buoyant Arabian plate lithosphere "choking" the subduction zone; buoyancy forces arising from thickened crust making it easier to shorten adjacent areas or transport crust laterally out of the collision zone.

[3] In the rest of the paper each part of the Arabia-Eurasia collision is described separately, moving roughly northward from the Arabian side of the collision into Eurasia. For each area we summarize the active slip rates, finite deformation and timing of initial deformation (Table 1). In the rest of this section we summarize current knowledge about these parameters for the collision zone as a whole.

[4] The present margins of the collision zone are well defined, picked out by cutoffs in topography and seismicity [*Jackson and McKenzie*, 1988] (Figures 1 and 2). Abrupt topographic fronts at the Persian Gulf and along the northern side of the Greater Caucasus and the Kopet Dagh define the southern and northern margins of major active deformation. The eastern boundary is formed by a series of north-south right-lateral faults in eastern Iran, which allow central Iran to move northward with respect to Afghanistan

Table 1. Deformation Rates Within the Arabia-Eurasia Collision Zone[a]

	Dead Sea Fault System	North Anatolian Fault	East Anatolian Fault	Turkish-Iranian Plateau	Greater Caucasus	Lesser Caucasus	Alborz	Alborz: Mosha Fault	Talesh	Kopet Dagh	South Caspian	Zagros Simple Folded Zone	Eastern Iran
Active deformation rate, mm yr^{-1}	2–8 l-l slip	24 ± 1 r-l slip	9 ± 1 l-l slip	<2 shortening	6 shortening	4 shortening - at northern side?	9? shortening	? l-l slip	?shortening	≤16 shortening	5? shortening	10 (NNE-SSW) convergence	≤16 r-l slip
Cumulative deformation, km	105 l-l slip	80–85 r-l slip	27–33 l-l slip	≤200 shortening	≥130 shortening	?	30 shortening	30–35 l-l slip	30 shortening	75 shortening	15 shortening	50 (NE-SW shortening)	80 r-l slip
Pliocene-Quaternary deformation, km	≤40	80–85	27–33	little thickening	?	?	≤30	≤30–35	≤30	75	15	50? (NE-SW shortening)	?
Start of deformation, Ma	≤20	5	3	≥12	>25	>7	~25?	≥5	~10	≥5	3–5	~5	?
Evidence for reorganization since late Miocene	not clear	focused deformation	start of faulting	not clear	increase in erosion and exhumation rates; magmatism	peneplanation; magmatism	granitoid exhumation; reversal of strike-slip; magmatism	none	not clear	onset of shortening?	onset of sediment folding; rapid subsidence	syn-fold sedimentation	none
Extrapolation of active deformation over 5 million years, km	10–40	120	45	<10	30	20	45?	–	–	≤80	25	50	≤80

[a]Derived from sources described in the text. Here l-l is left-lateral; r-l, right-lateral.

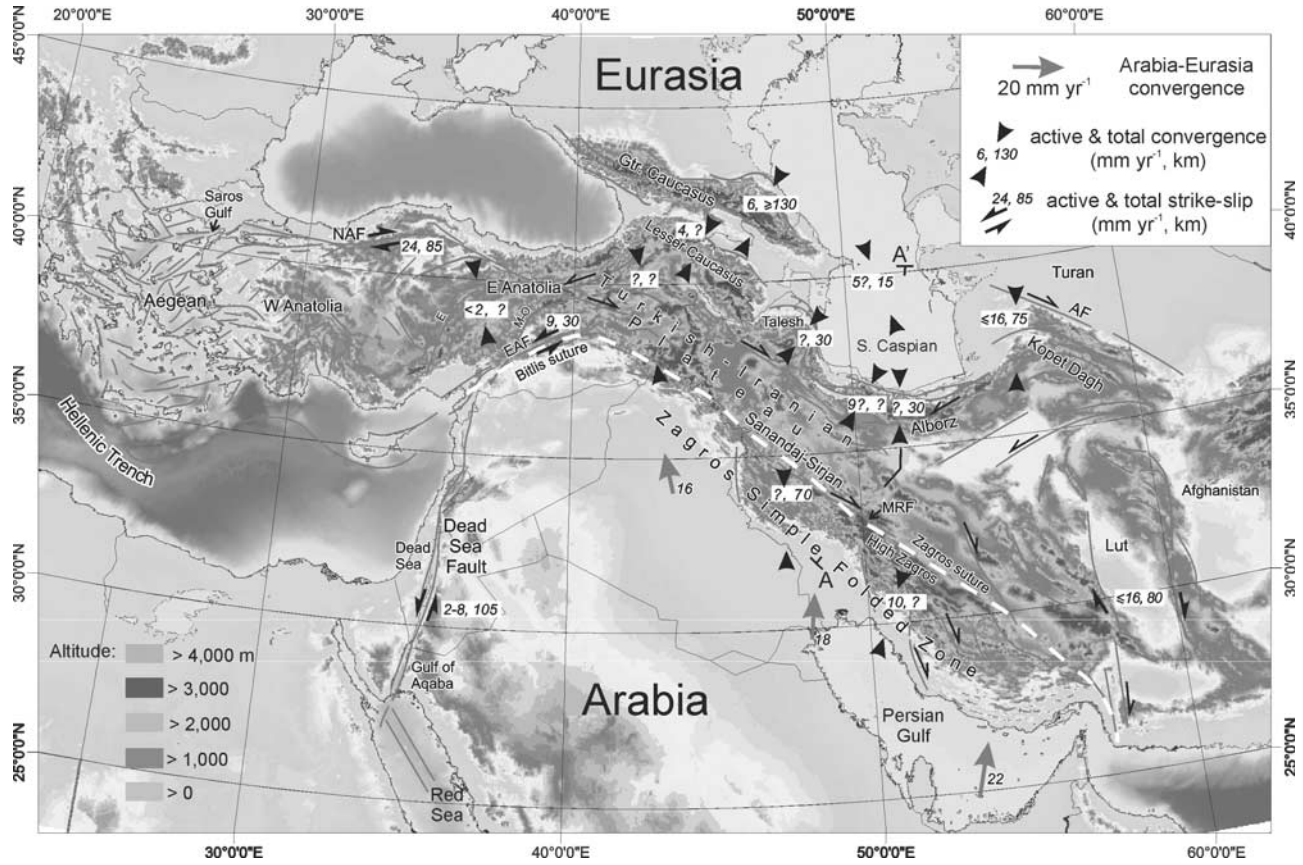

Figure 1. Topography, structure, current deformation rates and finite strain of the Arabia-Eurasia collision. Numbers in italics are present shortening or slip rate in mm yr^{-1}, followed by finite shortening or strike-slip in kilometers; see text for data sources for each area. Abbreviations are as follows: AF, Ashgabat Fault; E, Ecemiş Fault; EAF, East Anatolian Fault; M-O, Malatya-Ovacik Fault; MRF, Main Recent Fault; NAF, North Anatolian Fault. Red lines indicate main active faults, with thrusts marked by barbs. Present Arabia-Eurasia convergence rates from *Sella et al.* [2002]. A-A′ marks the section line of Figure 4. See color version of this figure at back of this issue.

(Figure 2). In the west, rapid extension in the Aegean occurs above the Hellenic subduction zone. Shortening and crustal thickening within the collision zone has produced mountain belts, principally the Greater Caucasus, Zagros, Alborz, Kopet Dagh and the Turkish-Iranian plateau (Figures 1 and 2). Strike-slip faulting is also prominent. The portion of Turkey between the North and East Anatolian faults is transported westward as these bounding faults slip with right- and left-lateral motion respectively [*McKenzie*, 1972].

[5] Active deformation rates in the Arabia-Eurasia collision zone are becoming better constrained through a combination of plate circuit and GPS studies [*DeMets et al.*, 1990, 1994; *Reilinger et al.*, 1997; *McClusky et al.*, 2000; *Sella et al.*, 2002; *Tatar et al.*, 2002]. A recent GPS-based global plate motion model [*Sella et al.*, 2002] gives lower estimates of the Arabia-Eurasia convergence rate than earlier, non-GPS models [*DeMets et al.*, 1990, 1994], typically by ~12 mm yr^{-1}. The GPS-derived velocity for the northern margin of the Arabian plate is 18 ± 2 mm yr^{-1} relative to Eurasia at longitude 48°E [*McClusky et al.*, 2000]. The convergence rate increases eastward because the Arabia-Eurasia Euler pole lies in the Mediterranean region, and is roughly 10 mm yr^{-1} higher in eastern Iran than in the west (Figure 1).

[6] Estimates for the age of the initial collision between Arabia and Eurasia vary markedly, from ~65 Ma [*Berberian and King*, 1981], using the end of ophiolite obduction, to ~5 Ma [*Philip et al.*, 1989], taking the onset of coarse clastic sedimentation around parts of the Greater Caucasus. Neither of these approaches provides a date for the first time continental crust came into contact from the converging plates. Deformation and syn-tectonic sedimentation took place on the northern side of the Arabian plate in the early Miocene (~16–23 Ma) [*Robertson*, 2000], related to the overthrusting of allochthonous nappes originating on the Eurasian side of Neo-Tethys. Other studies in the same region put the initial collision-related deformation as Oligocene [*Yılmaz*, 1993], or middle Eocene (~40 Ma) [*Hempton*, 1987]. Therefore 16–23 Ma is likely to be the minimum age range for initial plate collision. Suturing may have been diachronous from the Arabian promontory in the north, southeast along the Zagros [*Stoneley*, 1981]. Since initial collision along the Bitlis-Zagros suture, the Arabian plate has moved ~300–500 km northward with respect to

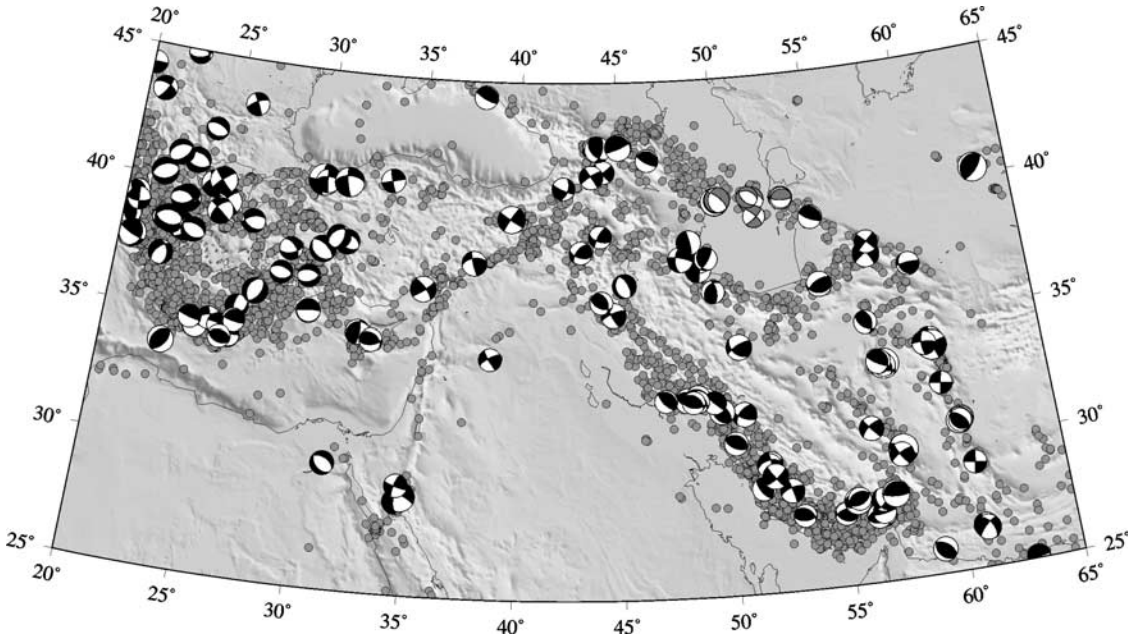

Figure 2. Best-double-couple CMT solutions from the Harvard catalogue (http://www.seismology.harvard.edu/CMTsearch.html) for earthquakes with depth $\leq$30 km, Mw $\geq$ 5.5 and double-couple component $\geq$70%, in the interval 1977–2001. Focal mechanisms in gray in the Caspian Sea are for earthquakes deeper than 30 km and are taken from *Jackson et al.* [2002]. Epicenters are from the catalogue of *Engdahl et al.* [1998]. Earthquakes deeper than 30 km associated with the subduction zones in the Makran and Hellenic Trench have been omitted.

stable Eurasia, based on an extrapolation of *Dewey et al.*'s [1989] Africa-Eurasia motion history to include the Arabian plate (Figure 3).

2. Zagros

[7] The Arabian plate passive margin is deformed southwest of the Zagros Suture, forming the Zagros mountains (Figures 1 and 4). The Zagros mark the present southern side to the broad collision zone, and the region's seismicity shows that it absorbs an important part of the overall convergence. The High Zagros lies between the original suture and the High Zagros Fault. This region is the most exhumed part of the Zagros, and in the northwest contains highly imbricated Arabian margin strata. Folds become more open to the southeast, indicating that the structure (and finite shortening?) of the High Zagros is not the same along strike [*National Iranian Oil Company*, 1975, 1977a]. Southwest of the High Zagros Fault, the Arabian margin strata are less imbricated at exposed levels, less exhumed, and form the classic whaleback anticlines of the Simple Folded Zone [*Falcon*, 1974].

[8] North-south convergence across the northwest Zagros is achieved through a combination of northeast-southwest shortening and right-lateral strike-slip faulting on the Main Recent Fault [*Talebian and Jackson*, 2002], which lies approximately along the suture trace (Figures 1 and 4). There are no other major, northwest-southeast, seismically active strike-slip faults within this part of the Simple Fold Zone that could help partition the overall convergence in this way. Further southeast, there is a zone of north-south trending right-lateral faults within the central Zagros. In the eastern part of the range the trend of folds and faults is closer to east-west. These roughly east-west structures accommodate the overall convergence without requiring a continuation of the Main Recent Fault, which dies out at $\sim$51°E.

[9] A GPS survey in the central Zagros indicates an active convergence rate in a NNE-SSW direction of 10 mm yr^{-1} across the central part of the Simple Folded Zone at longitude 52°E [*Tatar et al.*, 2002]. A similar amount of convergence ($\sim$10 mm yr^{-1}) must be taken up elsewhere in Iran, as the overall Arabia-Eurasia convergence at this longitude is $\sim$20 mm yr^{-1} [*Sella et al.*, 2002]. *Tatar et al.* [2002] found little evidence for active shortening within the High Zagros in this study, although their study had only three GPS stations in this region. This finding is consistent with the scarcity of seismic thrust events in the High Zagros [*Talebian and Jackson*, 2004].

[10] *Falcon* [1974] estimated the total shortening in the Simple Folded Zone as $\sim$30 km, but this is based on the assumption that Phanerozoic strata are concentrically folded above mobile salt, without significant shortening by thrust faulting. More recent work highlights the presence of seismically active basement thrusts [e.g., *Maggi et al.*, 2000] and recognizes thin-skinned thrusts within the deformed sediments [*Colman-Sadd*, 1978]. Right-lateral offset along the Zagros Main Recent Fault is about 50 km, based

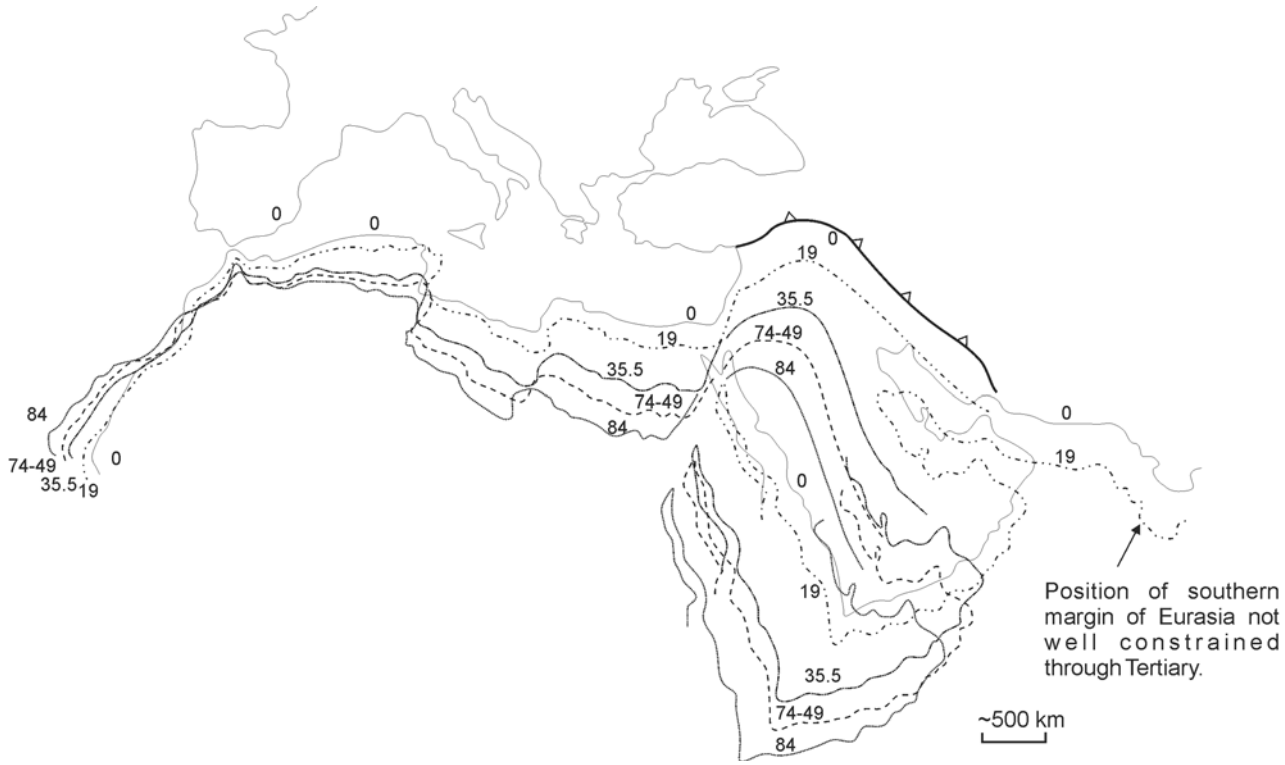

Figure 3. Plate reconstructions for the convergence of Africa-Arabia and Eurasia. Numbers are ages in Ma. Adapted from the Africa-Europe reconstructions of *Dewey et al.* [1989] by extending the continental margin to include Arabia, and allowing for ~100 km relative motion between Arabia and Africa post 20 Ma. There has been roughly 300–500 km of Arabia-Eurasia convergence since initial collision at 20–30 Ma. This is comparable with the convergence recognized within the collision zone.

on a restoration of offset drainage and geological markers along the fault from roughly 36°N 46°E to 32°N 51°E [*Talebian and Jackson*, 2002]. This implies ~50 km northeast-southwest shortening across the Zagros mountains to the southwest of the Main Recent Fault, and a total north-south convergence of ~70 km. A balanced and restored cross-section through the northwest Simple Folded Zone, between ~32°N 48.5°E and ~33°N 50°E suggests total northeast-southwest shortening is roughly 50 km [*Blanc et al.*, 2003], consistent with the estimate derived from the offset of the Main Recent Fault. *McQuarrie* [2004] produced balanced and restored cross-sections that include both the Simple Folded Zone and the High Zagros, and estimated 70 ± 20 km northeast-southwest shortening.

[11] Fold growth in the Simple Folded Zone of the Zagros was synchronous with deposition of Bakhtyari Formation conglomerates. These rocks are not well-dated, and were described as intra Pliocene by *James and Wynd* [1965] on the basis that there were no diagnostic fossils within the unit, but Pliocene fauna in the underlying Agha Jari Formation. These authors also stressed that the unit was likely to be diachronous. Initial fold development in many

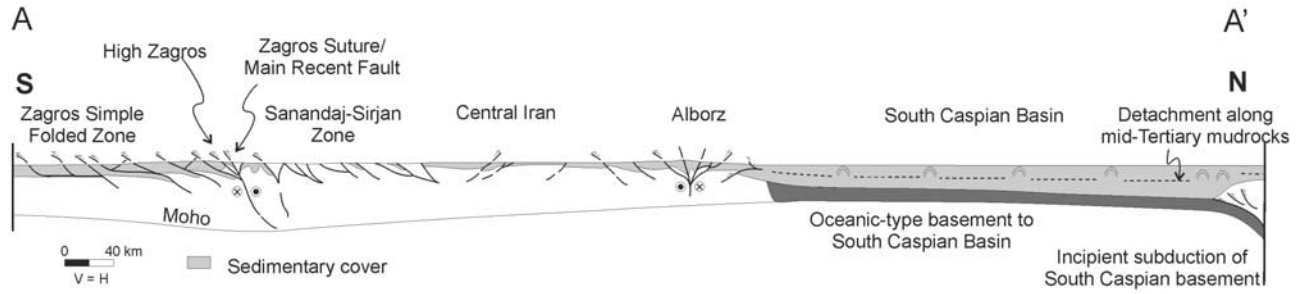

Figure 4. Cross section through the collision zone. Location shown on Figure 1. Geology derived from *National Iranian Oil Company* [1978]; *Alavi* [1994]; *Allen et al.* [2003a]; *Blanc et al.* [2003].

areas appears to pre-date the Bakhtyari Formation, given the angular unconformity between the Bakhtyari Formation and underlying strata [e.g., *O'B Perry and Setudehnia*, 1966]. Deformation in the High Zagros may also have begun before the Pliocene, because upper Miocene – lower Pliocene terrestrial clastics within the Simple Folded Zone thicken toward to the northeast and were derived from the same direction [*Elmore and Farrand*, 1981]. Little is known about the finite shortening or age of deformation within the High Zagros.

[12] The 10 mm yr^{-1} rate of active NNE-SSW convergence in the central Zagros Simple Folded Zone [*Tatar et al.*, 2002] would take ~7 million years to achieve the ~70 km of finite north-south convergence in the northwest Zagros Simple Folded Zone [*Talebian and Jackson*, 2002; *Blanc et al.*, 2003], although we note that this comparison is between different slightly azimuths. There is an assumption in this extrapolation that it is valid to use GPS-derived slip rates in comparison with long-term deformation patterns. There is no a priori evidence for this, but it is a useful starting point for such a large region, and similar comparisons are made at the end of following sections for other areas of the collision.

3. Dead Sea Fault System

[13] The Dead Sea Fault System (Figure 1) is important because it is the Arabia-Africa plate boundary and so records the motion between these plates. It consists of left-lateral fault segments that connect the active oceanic spreading centers in the Red Sea to the compressional deformation zones in southeast Anatolia and the Zagros [*Garfunkel*, 1981]. It has a total length of ~1000 km, and includes several pull-apart basins and push-up zones, formed in regions of overlap between left-stepping and right-stepping fault segments respectively. The most well known of the pull-aparts is the Dead Sea Basin [*Manspeizer*, 1985].

[14] GPS data [*McClusky et al.*, 2003] indicate ~6 mm yr^{-1} of relative Arabia/Africa motion in the northern Arabian platform. The local GPS survey of *Pe'eri et al.* [2002] gives a lower value for Dead Sea Fault slip: 2.6 ± 1.1 mm yr^{-1}. There is also a range in the estimates for Pliocene-Quaternary rates based on the offset of dated features. Offset late Pleistocene fans give a slip rate 4 ± 2 mm yr^{-1} for the sector between the Dead Sea and the Gulf of Aqaba [*Klinger et al.*, 2000]. *Ginat et al.* [1998] estimated 3–7.5 mm yr^{-1} from displaced Pliocene-Quaternary alluvial terraces in Wadi Aqaba, at the northern end of the Gulf of Aqaba. *Niemi et al.* [2001] estimated 4.7 ± 1.3 mm yr^{-1} since 15 Ka, from offset stream channels and fan surfaces south of the Dead Sea.

[15] The total offset of the Dead Sea Fault System, south of the Dead Sea, is ~105 km [*Quennell*, 1958]. A dolerite dyke swarm dated at 22–18 Ma shows the full 105 km offset, and so constrains the maximum age of initial faulting [*Eyal et al.*, 1981]. *Quennell* [1958] and *Manspeizer* [1985] suggested two phase movement, with ~40 km of offset in the Pliocene-Quaternary, or entirely in the Quaternary, based on the Pliocene-Quaternary age of sediments in the Dead Sea, but this is equivocal [e.g., *Sneh*, 1996].

[16] Summarizing these results, there is a wide range of estimates for the present left-lateral slip rate on the Dead Sea Fault System: ~2–8 mm yr^{-1}. There is too much spread in the data to compare short-term and long-term slip rates in detail. It would take ~13 million years to achieve the full 105 km offset if long-term motion took place at the top end of the range of active slip rates.

4. Turkish-Iranian Plateau

[17] The Turkish-Iranian plateau is one of the two main plateaux in the Alpine-Himalayan collision system, the other being Tibet [*Şengör and Kidd*, 1979; *Dewey et al.*, 1986]. It extends from eastern Anatolia to eastern Iran, and typically has elevations of ~1.5–2 km, decreasing to about 500 m in eastern Iran. Roughly half of the present collision zone lies within the plateau, much of which is internally drained.

[18] The basement of the plateau consists of microcontinents accreted to each other and Eurasia by the Late Cretaceous or early Tertiary [*Şengör*, 1990], interspersed with zones of ophiolites and mélanges. The microcontinents include the Sanandaj-Sirjan zone, parallel to and northeast of the later Zagros suture, and the Lut block in eastern Iran (Figure 1). The Mesozoic and Tertiary sedimentary cover of the Lut block is less deformed than surrounding areas. Volcanics of late Cretaceous – early Miocene age in the Sanandaj-Sirjan zone and central Iran represent Andean-type magmatism in southern Eurasia during Neo-Tethyan subduction [*Berberian et al.*, 1982]. Volcanic and turbidite successions up to 5 km thick represent Eocene back-arc extension across central Iran, the Alborz, the Lesser Caucasus and eastern Black Sea regions, north of the Neo-Tethyan subduction zone, and prior to Arabia-Eurasia collision [*Brunet et al.*, 2003]. This succession is commonly overlain in central Iran by terrestrial clastics, evaporites and volcanics of the Lower Red Formation, of Oligocene age [*Stöcklin*, 1971]. Marine deposition resumed across much of central Iran with the carbonates of the largely lower Miocene Qom Formation; similar lower Miocene marine strata were deposited across much of Anatolia and the Lesser Caucasus [*Şengör et al.*, 1985; *Toloczyki et al.*, 1994]. The Qom Formation pinched out in the north against the southern side of the Alborz and in the south along a line parallel to and ~100 km northeast of the Zagros suture [*Stöcklin*, 1971] – indicating sub-aerial relief both north and south of the marine basin. The end of marine sedimentation may have been diachronous: the Qom Formation is overlain by middle Miocene terrestrial clastics of the Upper Red Formation, but the youngest marine strata in eastern Anatolia are late middle Miocene, ~12 Ma [*Dewey et al.*, 1986].

[19] Seismicity [*Jackson et al.*, 1995]; (Figure 2) and GPS [*McClusky et al.*, 2000] data show that there is little active crustal shortening over most of the plateau (Figures 1 and 2), although ~4 mm yr^{-1} of shortening may take place across the Lesser Caucasus, at the northern side [*Reilinger et al.*, 1997; *McClusky et al.*, 2000]. There are prominent strike-slip faults, especially in eastern Anatolia and north-

west Iran (Figure 2) [*Talebian and Jackson*, 2002], but when these structures are considered in the overall velocity field they do not indicate eastward transport of the plateau out of the collision zone [*Jackson et al.*, 1995], in contrast to the well-documented westward transport between the North and East Anatolian faults. The Turkish-Iranian plateau is therefore important for understanding how strain has been accommodated over the long-term, but takes up little of the present Arabia-Eurasia convergence by shortening or lateral transport of crust eastward out of the convergent zone.

[20] There are few estimates for the total late Cenozoic shortening across the plateau. *Pearce et al.* [1990] suggested it could be as much as 200 km, based on estimates that the crust was ~30 km thick before shortening and ~50 km thick at present. Miocene strata are commonly folded and thrusted [e.g., *National Iranian Oil Company*, 1977b]. In many places these folded strata lie below undeformed volcanics mapped as upper Miocene to Quaternary in age, such as the extreme northwestern tip of Iran at 39.25°N 44.75°E, around Maku [*Geological Survey of Iran*, 1975], and southeast of the city of Tabriz at 37.25°N 47°E [*Geological Survey of Iran*, 1978]. An intra-Pliocene regional unconformity within the Lesser Caucasus separates younger, flat-lying strata and alkali volcanics from folded middle and upper Miocene calc-alkali volcanics and associated sediments; strike-slip faults cut dykes, thrusts and folds as young as 7 Ma [*Koçyigit et al.*, 2001]. There are also cases where post middle Miocene volcanics are recorded as folded or faulted (such as at ~37.4°N 47.3°E [*National Iranian Oil Company*, 1977b]), but there are fewer examples of this pattern.

[21] There are few well-constrained estimates of present crustal thickness, based on receiver function analysis. A study of the Lesser Caucasus in Armenia indicates the crust in that area is 64 ± 4.8 km thick [*Sandvol et al.*, 1998]. Thicknesses are lower to the southwest, in eastern Anatolia, at 40–50 km [*Zor et al.*, 2003], but still greater than normal for continental crust. There are also studies that estimate crustal thickness through other means, such as seismic refraction surveys and gravity modelling. *Snyder and Barazangi* [1986] found that the crust thickens from ~40 km at the Persian Gulf to ~65 km at the Zagros suture, while a recent review of the Middle East found that most of the Turkish-Iranian plateau is underlain by crust 45–50 km thick [*Seber et al.*, 2001]. Therefore the Turkish-Iranian plateau has thicker than average continental crust, consistent with the evidence for post late middle Miocene crustal shortening, but the exact amount of shortening and overall crustal thickness are not well-constrained.

[22] Surface uplift of the plateau has been suggested to be a regional event [*Şengör and Kidd*, 1979], rather than a progressive process associated with a migrating deformation front. This is based on the apparent uniformity of timing and elevations attained by an erosion surface, proposed as late Miocene – early Pliocene in age [*Şengör and Kidd*, 1979], but not well-dated.

[23] In summary, the Turkish-Iranian plateau was shortened, thickened and elevated since ~12 Ma at the latest, during or prior to regional magmatism. This has produced crust locally up to ~64 km thick [*Sandvol et al.*, 1998], in a region where there are Miocene marine strata [*Toloczyki et al.*, 1994]. There is little evidence for active regional shortening and crustal thickening in the seismicity or GPS data. It is not known precisely when crustal thickening ended, and whether there was a gradual or sudden switch to shortening in the active fold and thrust belts north and south of the plateau.

5. Eastern Iran

[24] The eastern limit of Arabia-Eurasia deformation occurs at roughly longitude 61°E, close to the political border between Iran and Afghanistan. Further east there is a sharp cut-off in seismicity, mountainous topography and active fault activity (Figures 1 and 2).

[25] The 10 mm yr^{-1} convergence in the central Zagros [*Tatar et al.*, 2002] is likely to be a minimum value for the eastern Zagros, given that the width of the range and the total Arabia-Eurasia convergence rate increase eastward. Therefore, using an Arabia-Eurasia convergence rate of 26 mm yr^{-1} at longitude ~60°E [*Sella et al.*, 2002], a maximum of ~16 mm yr^{-1} remains to be accommodated between central Iran and stable Eurasia. This must result in a comparable amount of right-lateral shear on north-south strike-slip faults along the eastern margin of Iran (Figure 5). North of latitude 34°N, this right-lateral shear is accommodated by east-west left-lateral faults that rotate clockwise about vertical axes (Figure 5a) [e.g., *Jackson and McKenzie*, 1984].

[26] The maximum of 16 mm yr^{-1} of right-lateral shear is divided between the Gowk-Nayband and Sistan Suture Zone fault systems that occur along the western and eastern margins of the Dasht-e-Lut respectively (Figure 5a). These systems each contain several parallel fault strands. However, little is known of the slip-rates across these faults, and hence the present-day distribution of strain.

[27] *Walker and Jackson* [2002] used drainage systems and structural features displaced by the Gowk fault to estimate a total cumulative offset of ~12 km. The Gowk fault is the only active strike-slip fault west of the Dasht-e-Lut at that latitude (Figure 5a), and so the majority of right-lateral shear west of the Dasht-e-Lut is expected to be localized across it. Displacement of distinctive bed-rock lithologies by active faults in the Sistan Suture Zone indicate a minimum of ~70 km of cumulative right-lateral slip east of the Dasht-e-Lut, based in part on initial observations by *Freund* [1970], and *Tirrul et al.* [1983] (Figure 5b).

[28] A minimum of ~80 km of right-lateral shear between central Iran and Afghanistan is required by summing these estimates of cumulative fault slip. This would take ~5 million years to achieve at the likely 16 mm yr^{-1} maximum rate of active right-lateral shear. More work is needed to constrain directly both the active slip rates and time of initial deformation.

6. East and North Anatolian Faults

[29] Westward transport of the Anatolian (Turkish) plate occurs by slip on the East and North Anatolian faults

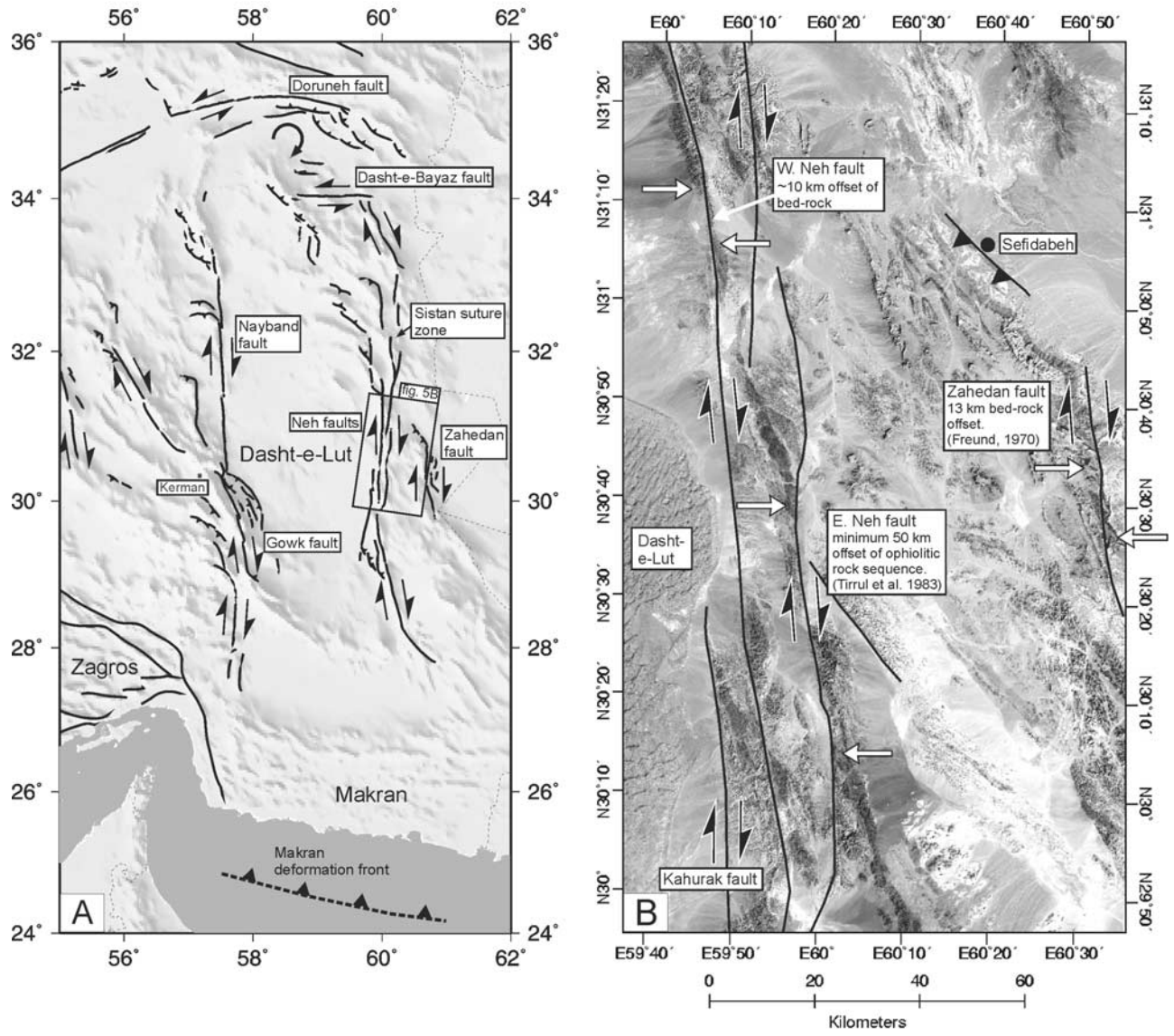

Figure 5. (a) Detailed fault map of eastern Iran. Active right-lateral strike-slip faults accommodate shear between central Iran and Afghanistan. The box shows the location of Figure 5b. (b) Landsat TM image of part of the Sistan Suture Zone. Three right-lateral strike-slip faults, with a combined bed-rock displacement of ~70 km are seen at latitude 30.7°N.

[*McKenzie*, 1972]. The quality of the data on the history and present slip rates of these faults provides important constraints on both the short-term and long-term deformation patterns in this part of the collision.

[30] The left-lateral East Anatolian Fault accommodates motion between the Arabian and Anatolian plates (Figure 1). It trends for ~400 km southwest of its intersection with the North Anatolian Fault at Karliova, at approximately 39.5°N 41°E. There are several strands to the fault zone, with localized pull-apart basins and push-up zones [*Lyberis et al.*, 1992; *Westaway*, 1994].

[31] Historical slip rates based on seismic moments of earthquakes along the East Anatolian Fault are 6–10 mm yr^{-1} [*Taymaz et al.*, 1991]. The GPS-derived slip rate is 9 ± 1 mm yr^{-1} [*McClusky et al.*, 2000]. There is considerable variation in published estimates of the overall offset. The higher end of the range is 27–33 km [*Westaway and Arger*, 1996], constrained by offset geological markers, and by the length of the Golbasi strike-slip basin (~33 km). Other values in the order of 15–22 km [*Hempton*, 1985; *Dewey et al.*, 1986] may underestimate the total because they are based on offset drainage or geological features on individual fault segments [*Westaway and Arger*, 1996].

[32] Initial movement on the East Anatolian Fault is late Pliocene (~3 Ma) or younger [*Şaroglu et al.*, 1992; *Westaway and Arger*, 2001], based on the offset of volcanics

of this age. This refines earlier estimates that the fault began at ~5 Ma, based on the estimated Pliocene age of sediments in related basins [*Şengör et al.*, 1985] and the assumption that the East and North Anatolian Faults began their motion at the same time [*Dewey et al.*, 1986]. Several other, perhaps inactive, left-lateral faults have been identified in eastern Turkey, with slip on the order of tens of kilometers. These include the Malatya-Ovacik Fault [*Westaway and Arger*, 2001], with ~29 km offset between 5 and 3 Ma, and the Ecemiş Fault [*Jaffey and Robertson*, 2001], with ~60 km offset since the late Eocene, but mainly pre-Pliocene.

[33] The estimates for the slip rate, finite offset and timing of the East Anatolian Fault are in good agreement: 9 ± 1 mm yr^{-1} for 3 million years suggests 24–30 km of finite offset, compared with the 27–33 km of offset estimated from the geology.

[34] The right-lateral North Anatolian Fault accommodates slip between the Eurasian and Anatolian plates over a length of >1200 km (Figures 1 and 2). Its eastern limit lies at the Karliova triple junction. The fault splits into several strands where it enters the north Aegean. The GPS-derived slip rate for the North Anatolian Fault is 24 ± 1 mm yr^{-1} [*McClusky et al.*, 2000].

[35] Displacement in the western part of the North Anatolian Fault (Saros Gulf) has been constrained by offset folds as ~85 km since ~5 Ma [*Armijo et al.*, 1999] (however, see *Yaltırak et al.* [2000]). This is similar to the drainage offsets restored by 80–100 km between 30° and 38°E by *Westaway* [1994] and the 85 ± 5 km offset of a Tethyan suture reported at 38°E by *Seymen* [1975]. Other, shorter offsets are summarized by *Barka* [1992], and longer estimates by *Bozkurt* [2001], but ~80–85 km is emerging as a consensus figure for most of the length of the fault zone [*Barka et al.*, 2000; *Bozkurt*, 2001].

[36] There is evidence for distributed strike-slip and/or extension within regions now cut through by the North Anatolian Fault [e.g., *Tüysüz et al.*, 1998; *Coskun*, 2000]. *Barka and Hancock* [1984] suggested that a broad right-lateral shear zone operated toward the end of the Tortonian (~7 Ma), replaced by activity along the present main strand of the North Anatolian Fault in the early Pliocene. *Bozkurt* [2001] also concluded that faulting began at ~5 Ma, based on a review of studies of individual sections of the fault zone. One place where there is a precise age for the onset of deformation is the Adapazarı pull-apart basin, along the west of the fault zone at ~40.7°N 30.5°E: rodent fossils date the onset of sedimentation in this fault-related basin as latest Pliocene [*Ünay et al.*, 2001].

[37] In summary, a long-term extrapolation of the GPS-derived slip rate along the North Anatolian Fault (24 ± 1 mm yr^{-1}) would achieve the finite offset of 80–85 km in ~3.5 million years [*McClusky et al.*, 2000], less than the ~5 million years estimated for activity along the modern fault trace.

7. Alborz

[38] The Alborz range in northern Iran is roughly 600 km long and 100 km across, running along the southern side of the Caspian Sea (Figure 1). Active, range-parallel, left-lateral strike-slip faults trend ENE in the east of the Alborz, WNW in the west, as far west as 49°E [*Berberian*, 1997; *Jackson et al.*, 2002; *Allen et al.*, 2003a]. Roughly north-south shortening takes place via thrusts which dip inward from both sides of the range (Figure 4). Sedimentary and volcanic rocks of ages from late Precambrian to Quaternary are involved in the deformation. Igneous intrusions are rare, but there both early and late Tertiary granitoids [*Axen et al.*, 2001]. Unequivocal Precambrian basement is not exposed. The active thrusting contrasts with the relative lack of activity in central Iran to the south, and shows that Arabia-Eurasia convergence takes place north as well as south of the Turkish-Iranian plateau. The range has summits over 4000 m, but crustal thicknesses are reportedly surprisingly low for such mountainous terrain, at ~35 km [*Tatar*, 2001].

[39] At present there are no published GPS-based estimates for the shortening rate or strike-slip rate within the Alborz. If the overall Arabia-Eurasia convergence at the longitude of the Alborz is ~20 mm yr^{-1} [*Sella et al.*, 2002] and ~10 mm yr^{-1} of this is accommodated in the Zagros [*Tatar et al.*, 2002], the convergence across the combined Alborz and South Caspian Basin should be roughly ~10 mm yr^{-1} – discounting any small component from central Iran. This is substantially less than the 15–20 mm yr^{-1} assumed by *Jackson et al.* [2002] based on earlier NUVEL 1A plate circuit values [*DeMets et al.*, 1990, 1994], which are now known to be too high [*Sella et al.*, 2002]. *Jackson et al.* [2002] described how the motion between the South Caspian and Iran and between the South Caspian and Eurasia takes place along azimuths of roughly 210° and somewhat north of 300°, respectively. Using these azimuths, but a value for the overall Iran-Eurasia convergence of ~10 mm yr^{-1}, the resultant velocity triangle shows roughly 9 mm yr^{-1} convergence across the Alborz and 5 mm yr^{-1} between the Caspian and Eurasia.

[40] Total north-south shortening across the Alborz is ~30 km (25–30%) at the longitude of Tehran, roughly 51.5°E, based on a structural cross-section [*Allen et al.*, 2003a]. This is a minimum estimate. Restoration of a truncated anticline shows that the eastern Mosha Fault has a left-lateral offset of ~30–35 km at 35.75°N 52°E [*Geological Survey of Iran*, 1987; *Allen et al.*, 2003a].

[41] *Axen et al.* [2001] documented ~5–7 km of exhumation in the north central Alborz since ~7 Ma, presumably caused by the onset or acceleration of compressional deformation in the range. The range-parallel left-lateral strike-slip faulting may have begun at this time. There are no indications of active range-parallel right-lateral faulting, but this occurred before 7 Ma. Pliocene-Quaternary strata on either side of the Alborz and within intermontane basins are non-marine clastics, and the successions generally coarsen up-section [*Stöcklin*, 1971]. However, coarse continental clastics of presumed Oligo-Miocene age (~25 Ma) were deposited in intermontane basins in the western Alborz [*Annells et al.*, 1975], indicating at least some mid Tertiary sub-aerial relief.

[42] If the present likely Alborz shortening rate of ~9 mm yr^{-1} was maintained it would account for all of

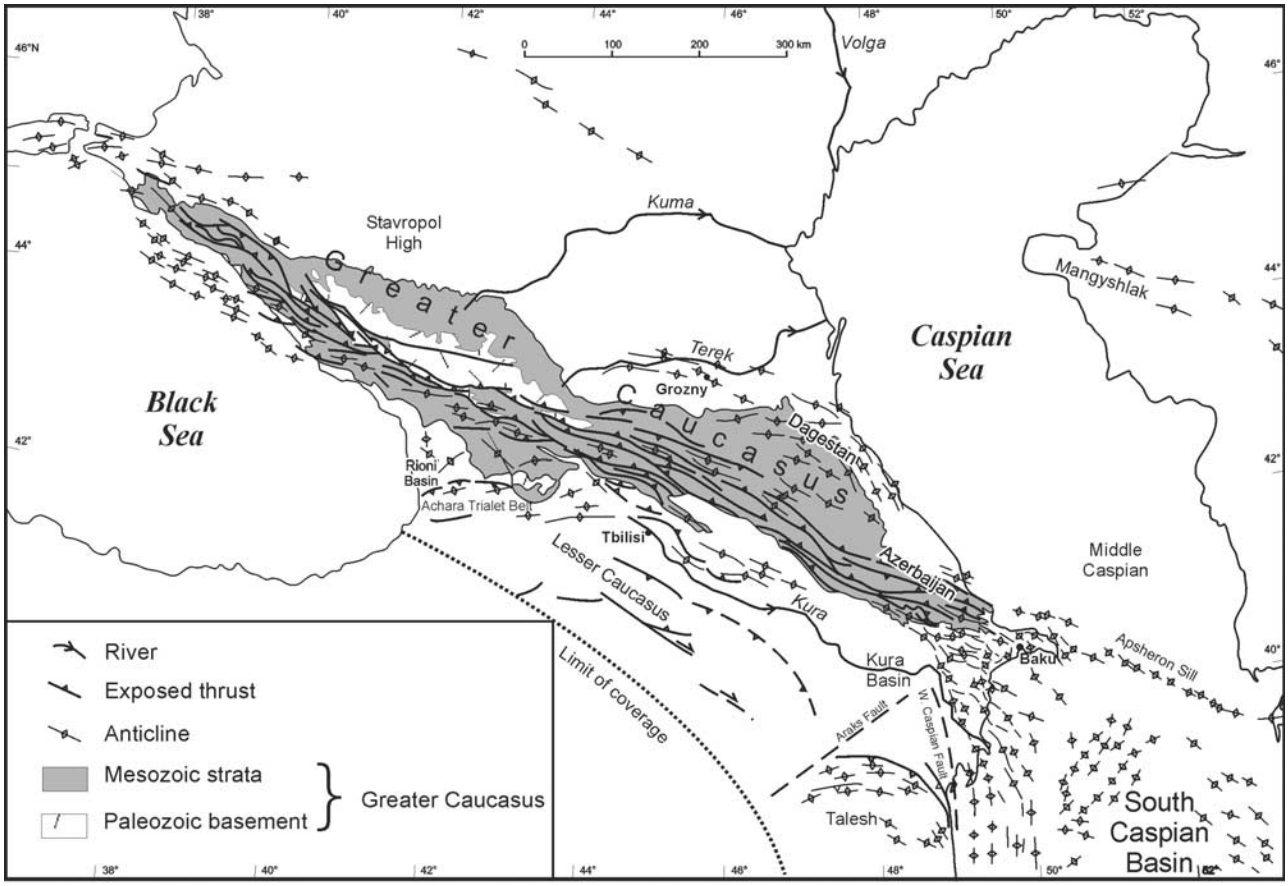

Figure 6. Structure of the Greater Caucasus, Talesh, western South Caspian Basin and the northeast side of the Lesser Caucasus. Compiled from several sources, principally *Nalivkin* [1983] and *Yakubov and Alizade* [1971].

the estimated finite shortening within 3–4 million years. This is a shorter time than since the late Miocene (7 Ma) age for the onset of rapid exhumation [*Axen et al.*, 2001] and much less than the Oligo-Miocene age of initial Cenozoic sub-aerial relief in the range.

8. Talesh

[43] The Talesh (Talysh) is an arcuate fold and thrust belt in northwest Iran and Azerbaijan (Figure 6), which deforms Paleogene volcanics and deep marine clastics and a Neogene succession that broadly shallows upward [*Allen et al.*, 2003b]. Summits reach ~2000 m at the Iran-Azerbaijan border, but the foreland of the range is below sea level at the margin of the Caspian Sea. Seismogenic thrusts at the eastern side of the range trend north-south, dip very gently west, and have hypocenters in the depth range of 15–27 km [*Jackson et al.*, 2002], showing that the basement to the Talesh presently overthrusts the South Caspian Basin to the east (Figures 2 and 6).

[44] There are no published geodetic results for the active convergence rate across the Talesh. Total shortening across the northeast of the Talesh is estimated at ~30 km, based on a restoration of folds and thrusts [*Jackson et al.*, 2002]. This is a similar value to the estimate for the Alborz to the southeast. There is no conclusive evidence for the time of initial compressional deformation, but strata from around the middle-late Miocene boundary (~10 Ma) display evidence for gravity flow processes [*Vincent et al.*, 2002], which indicates significant relief at this time. Pliocene-Quaternary strata are folded at the northern margin of the range, indicating young deformation [*Geological Survey of Iran*, 1994].

[45] Unfortunately, there are not enough data for the Talesh to compare short and long term deformation rates. Its structure shows that there is active shortening north of the Turkish-Iranian plateau, and that deformation in this part of the collision zone is very three-dimensional.

9. Kopet Dagh

[46] The Kopet Dagh trends at 120°–300° for 700 km through northeast Iran and Turkmenistan between the Caspian Sea and the Afghanistan border (Figure 1). It separates the Turan region from central Iran, and so shows how plate convergence happens at the northern side of the collision zone. The range is up to 3000 m in altitude, some 2000 m higher than the Turkmen foreland to the north. Jurassic-

Miocene marine carbonates and clastics were deposited across a region now deformed into a series of folds and thrusts. The range is much broader in the west than the east, which may mean it rotates clockwise about its eastern limit. The right-lateral Ashgabat Fault lies at the northern margin of the range [*Trifonov*, 1978]. This fault also has a component of thrust motion to the north [*Priestley et al.*, 1994].

[47] There are no published GPS results for the Kopet Dagh. If the north-south convergence rate in the eastern Zagros is at least the same as the central part ($\sim$10 mm yr^{-1}), as argued above, it implies that the Kopet Dagh convergence may be $\sim$16 mm yr^{-1} at maximum, if the *Sella et al.* [2002] estimate of the overall Arabia-Eurasia convergence at this latitude is correct.

[48] North-south shortening across the west of the range may be $\sim$75 km, based on a line balanced section by *Lyberis and Manby* [1999]. This represents $\sim$30% shortening of the 250 km wide western Kopet Dagh region. Further east, this is resolved into compression orthogonal to the Ashgabat Fault and right-lateral slip along it. *Lyberis and Manby* [1999] suggested that this shortening is principally Pliocene-Quaternary in age, based on the deposition of 4.5 km of Pliocene-Quaternary terrestrial clastics over an Oligocene-late Miocene marine succession. Uplift was apparently diachronous from east to west, based on Pliocene strata being marine in the west but non-marine in the east [*Lyberis and Manby*, 1999]. However, *Stöcklin* [1971] noted Neogene red bed clastics in the Iranian Kopet Dagh, which may imply that deformation, sub-aerial relief and terrestrial sedimentation all began before the Pliocene.

[49] If the likely maximum convergence rate of $\sim$16 mm yr^{-1} is representative of long-term deformation rates, it would take $\sim$5 million years to achieve the $\sim$75 km of total crustal shortening estimated for the range.

10. South Caspian Basin

[50] The basement to the South Caspian Basin has the geophysical properties of unusually thick oceanic crust or thinned, high-velocity continental crust [*Neprochnov*, 1968; *Mangino and Priestley*, 1998]. This basement is not exposed, being covered by a $\sim$20 km thickness of sedimentary rocks (Figure 4), about half of which is of Pliocene-Quaternary age [*Ali-Zade et al.*, 1985]. Little is known of the pre-Oligocene stratigraphy, but the Oligocene-lower Pliocene succession shallows upward, culminating in the thick (up to 6 km) Productive Series, which was deposited in fluvial, lacustrine and deltaic settings [*Devlin et al.*, 1999]. The age and original tectonic setting of the basement are not certain [*Brunet et al.*, 2003], but it is likely that the South Caspian originated as a back-arc basin at some time in the Jurassic-Paleogene interval.

[51] The interior of the South Caspian Basin is relatively aseismic, compared with the mountain ranges around it [*Priestley et al.*, 1994; *Jackson et al.*, 2002]. Earthquakes at depths of $\sim$80 km along its northern side (Figure 2) suggest northward underthrusting/subduction beneath the middle Caspian region. This cannot have been happening for a geologically long time, as the northern margins of the Greater Caucasus and Kopet Dagh are approximately colinear with the Apsheron Sill. This is a kinematically unstable configuration, given the opposite polarity of deformation within the onshore and offshore regions, and cannot persist for long [*Jackson et al.*, 2002]. Backstripping the stratigraphy of the northwest of the basin indicates $\sim$2.4 km of tectonic subsidence in the Pliocene and Quaternary [*Allen et al.*, 2002], interpreted as the result of this young subduction.

[52] Anticlines in the South Caspian Basin have a variety of orientations (Figure 6). A linear zone of folds at the north side of the basin form the Apsheron Sill, and presumably relate to deeper underthrusting of South Caspian basement beneath the middle Caspian. North-south folds at the western side of the basin relate to basement underthrusting to the west, beneath the Talesh. There may not be direct fault links between basement and cover. The anticlines are buckle structures, which are detached from the basement along mud-prone horizons within the thick sedimentary basin fill [*Devlin et al.*, 1999]. The overall strain is unlikely to be high, given the lack of evidence for major imbrication or crustal thickening. Line-balancing across each fold shows only a few percent shortening [*Devlin et al.*, 1999], and we extrapolate this across the basin to give a very approximate estimate of $\sim$5% visible north-south shortening in the supra-detachment cover, equivalent to $\sim$15 km shortening overall.

[53] Stratal pinchouts onto offshore folds are visible in late Pliocene and younger strata, indicating that folding began at $\sim$3.4 Ma [*Devlin et al.*, 1999]. Deformation in adjacent onshore folds may have begun $\sim$2 million years earlier [*Aliev*, 1960], given pinchouts onto folds in latest Miocene-early Pliocene strata.

[54] In summary, synchronous deposition and deformation of the South Caspian sedimentary cover of the South Caspian Basin in the last 3–5 million years is consistent with incipient subduction of its rigid basement northward under the middle Caspian region. The South Caspian region is unlikely to accommodate a major part of the Arabia-Eurasia convergence. If the South Caspian-Eurasia motion is $\sim$5 mm yr^{-1}, as described above in the section on the Alborz, it could achieve the 15 km of shortening estimated in the basin fill in 3 million years.

11. Greater Caucasus

[55] The Greater Caucasus range lies northeast of the Black Sea and northwest of the South Caspian Basin (Figure 6). It lies along trend from the Kopet Dagh, and also represents the zone of active deformation at the northern side of the Arabia-Eurasia collision.

[56] The present structure of the Greater Caucasus indicates major late Cenozoic shortening and inversion of a Mesozoic - lower Tertiary basin. The Moho under the range is at depths of up to 60 km [*Ruppel and McNutt*, 1990]. Palaeozoic basement is exposed in dominantly southward-directed thrust slices west of $\sim$44°E. Mesozoic strata are present in tight or isoclinal folds across the range all around the exposed Palaeozoic core [*Rogozhin and Sholpo*, 1988;

Allen et al., 2003b]. These folds are commonly associated with thrusts. The vergence of these structures is predominantly toward the south. However, there are north-directed structures on the northern margin, especially in the northeast (Dagestan). Pliocene-Quaternary strata are folded into elongate, linear, south-vergent anticlines on the southern side of the range, between the extant Kura and Rioni basins. Fault plane solutions show a predominance of thrusts that dip toward the range interior [*Philip et al.*, 1989; *Triep et al.*, 1995; *Jackson et al.*, 2002]. Late Cenozoic magmatism in the range is Pliocene and Quaternary in age [*Gazis et al.*, 1995].

[57] GPS studies across both the Greater and Lesser Caucasus provide a minimum north-south shortening rate of 10 ± 2 mm yr^{-1} [*Reilinger et al.*, 1997], of which ~60% is estimated to occur across the Greater Caucasus [*McClusky et al.*, 2000]. These studies estimate overall shortening rates, but not where it occurs within the range. Larger magnitude earthquakes are concentrated at the margins of the range, with epicenters predominantly in regions at altitudes of 1000 m or less (Figures 2 and 6 [*Jackson*, 1992]). There is less seismicity in the west of the range, where the crystalline basement is exposed.

[58] Estimates of overall shortening across the Greater Caucasus vary greatly, and we are not aware of published balanced and restored cross-sections. *Dotduyev* [1986] suggested ~200 km across a 100 km long traverse through the central Caucasus, which represents ~66% shortening. This seems high, given the preservation of unmetamorphosed Mesozoic-Cenozoic strata across much of the range, but is consistent with the range of 200–300 km deduced by *Ershov et al.* [2003] on the basis of simple area balancing restoration of the whole crust in a transect at ~44°E. *Sobornov* [1994] calculated 30–50 km (~25–40%) shortening across the Dagestan thrust belt in the northeastern Greater Caucasus, based on restoration of thrust sheets in the Mesozoic-Cenozoic strata. If these Dagestan values are representative for the entire range, they imply roughly 130 km of shortening where the range is presently 200 km across.

[59] Stratigraphic evidence (e.g., olistostrome deposits) is interpreted to mean compressional deformation within the Greater Caucasus during the late Eocene [*Banks et al.*, 1997], and so may pre-date the initial continental collision. Oligo-Miocene strata on the central northern side of the range thicken southward, unlike underlying units [*Ershov et al.*, 2003]: this may represent initial foreland basin development, and hence thrusting within the range. In the northeastern Greater Caucasus (Dagestan), there was a switch in paleocurrent direction from southwest- to northeast-directed in the late middle Miocene [*Sobornov*, 1994]. Upper Miocene shallow marine strata in the eastern Greater Caucasus (Azerbaijan) are folded and exposed [*Azizbekov*, 1972]. Provenance data for the uppermost Miocene-Pliocene succession in the northwest of the South Caspian Basin show an increase in the proportion of sand derived from the Greater Caucasus within this interval [*Morton et al.*, 2003]. Summarizing these data, there is evidence for mid-Tertiary uplift, foreland basin development and presumably deformation of the Greater Caucasus; the area involved has apparently increased over time.

[60] The Greater Caucasus is an area of the collision where the present shortening rate cannot account for all the observed strain in a few million years: the present shortening rate (~6 mm yr^{-1}) needs to be extrapolated for ~22 million years to account for the lower estimate for the finite shortening (~130 km). Thirty to 50 million years would be needed to account for the shortening estimates of 200–300 km at this rate.

12. Discussion

[61] Extrapolating present-day deformation rates for 3–7 million years produces displacements that equal or exceed the total deformation on many of fault systems currently active in the Arabia-Eurasia collision zone, including the Zagros Simple Folded Zone, the North and East Anatolian faults, the South Caspian Basin and the Alborz and Kopet Dagh ranges (Table 1). This age range is much shorter than the overall age of the collision, which began in the early Miocene (16–23 Ma) or earlier [*Hempton*, 1987; *Yılmaz*, 1993; *Robertson*, 2000]. It seems that the collision zone has not absorbed the overall plate convergence in the same way throughout its history, unless for some unknown reason slip rates on the active fault systems are consistently higher than long-term averages.

[62] There may have been a regional reorganization of the collision at ~5 ± 2 Ma, as suggested by several authors [e.g., *Wells*, 1969; *Quennell*, 1984; *Westaway*, 1994; *Axen et al.*, 2001]. This is the time when deformation started or intensified in many of the currently active regions, such as the East and North Anatolian faults, the South Caspian Basin and possibly the Kopet Dagh [*Barka et al.*, 2000; *Westaway and Arger*, 2001; *Devlin et al.*, 1999; *Lyberis and Manby*, 1999]. This is also the timeframe of rapid exhumation in the Alborz [*Axen et al.*, 2001], and initial deposition of the Bakhtyari Formation within the deforming Zagros Simple Folded Zone [*James and Wynd*, 1965]. Suggestions for the cause of this reorganization include the opening of the Red Sea [*Wells*, 1969], the arrival of buoyant Arabian lithosphere "choking" the Neo-Tethyan subduction zone [*Axen et al.*, 2001], the final closure of oceanic basins within Iran [*Jackson et al.*, 2002] and the elevation of the Turkish-Iranian plateau [*Allen et al.*, 2002].

[63] Oceanic spreading in the Red Sea would only cause reorganization of the Arabia-Eurasia collision if convergence rates increased, but there is no strong evidence for this in the history of the Dead Sea Fault System or the Red Sea [*Sneh*, 1996; *McQuarrie et al.*, 2003]. Nor is it obvious why an increase in convergence should require a reorganization of deformation within the collision zone, rather than an increase in strain rates on existing fault systems. It is not proven that there was a change in the nature of the Arabian lithosphere entering the collision zone at the end of the Miocene; more work is needed on the High Zagros to examine this idea. In any case, late Miocene terrestrial clastics within the Simple Folded Zone were derived from the northeast [*Elmore and Farrand*, 1981], suggesting that

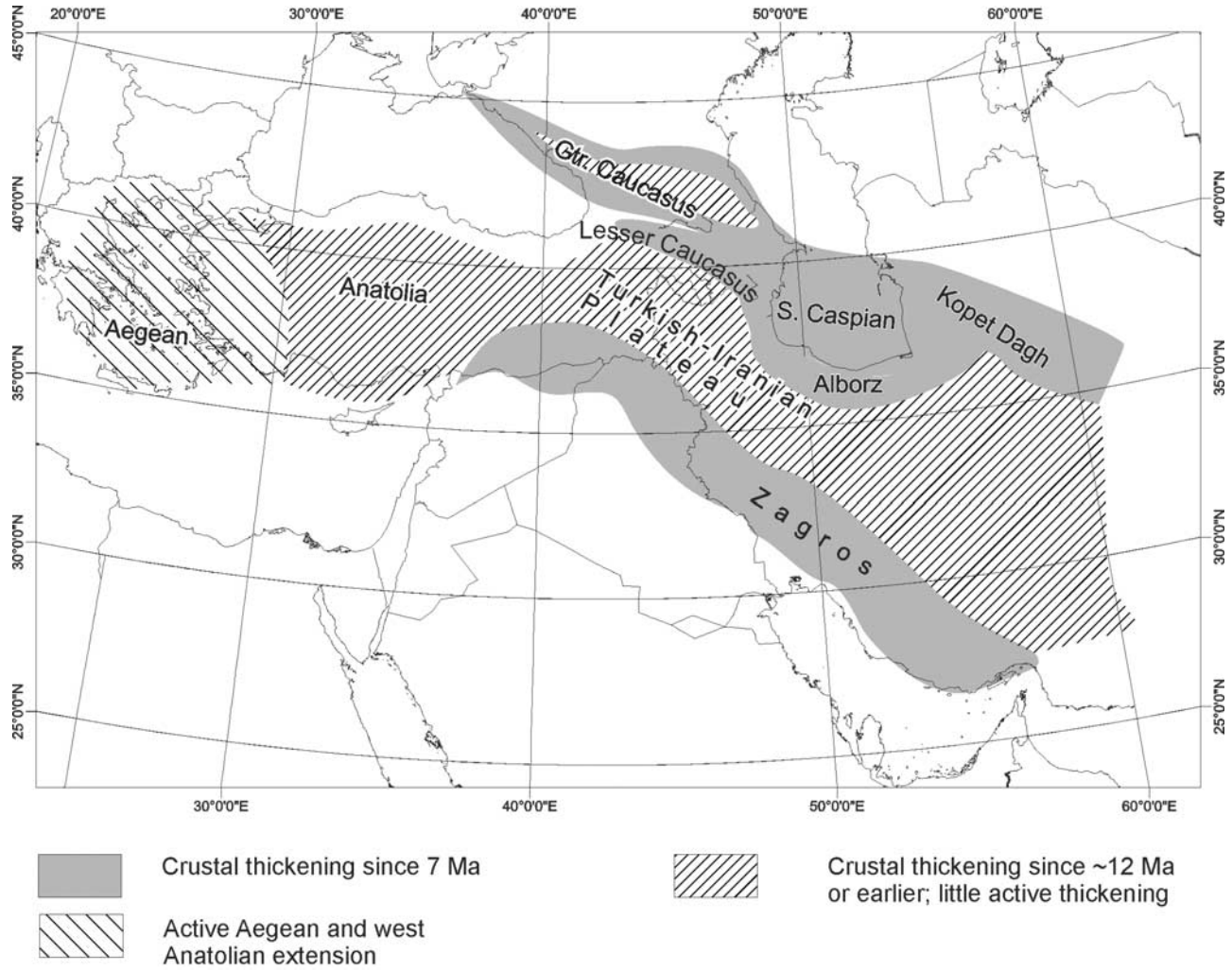

Figure 7. Pattern of deformation across the Arabia-Eurasia collision, highlighting areas where crustal thickening occurred since 12 Ma but not significantly at present (Turkish-Iranian plateau and interior of the Greater Caucasus), and mainly since ~7 Ma (Zagros Simple Folded Zone, Alborz, South Caspian Basin, Kopet Dagh, and Greater Caucasus foothills).

the Arabian plate was solidly docked to Eurasia before the Pliocene. If there were oceanic basins within Iran as recently as the middle-late Miocene, they have yet to be identified.

[64] Seismogenic thrusts (Figure 2) and GPS data show that active shortening is concentrated both north and south of the Turkish-Iranian plateau. The Turkish-Iranian plateau has little evidence for internal shortening at present, but must have undergone shortening, thickening and surface uplift since 12 Ma, which is the age of the youngest recorded marine sediments within it [*Dewey et al.*, 1986]. Parts of the Sanandaj-Sirjan zone and the Alborz were subaerially exposed before 12 Ma, given the pinch out of the lower Miocene Qom Formation against the margins of these regions [*Stöcklin*, 1971]. The Greater Caucasus, which was uplifted and presumably deforming in the mid-Tertiary or earlier [*Mikhailov et al.*, 1999], is presently shortening at ~6 mm yr^{-1} [*McClusky et al.*, 2000]. The range has poorly-constrained finite shortening (but ~130 km is the lower range of estimates), and thick crust (up to ~60 km [*Ruppel and McNutt*, 1990]). Earthquakes are concentrated at lower elevations, below 1000 m, and away from the crystalline basement. This suggests that shortening is focused at the range margins, and not higher, more exhumed, regions, and may mean that shortening in the Greater Caucasus migrates into its forelands once thick crust has been achieved. It is not clear whether this change has occurred gradually since the mid-Tertiary, or by abrupt reorganization(s). The Pliocene is a candidate time for a reorganization, given the onset of magmatism within the range [*Gazis et al.*, 1995] and the increased contribution of sand from the Greater Caucasus deposited in the adjacent South Caspian Basin [*Morton et al.*, 2003]. Therefore the Greater Caucasus is similar to the Turkish-Iranian plateau in several ways: seismicity, and presumably shortening, is focused on lower altitude areas at its margins, present convergence rates across the range

are inadequate to account for total shortening and crustal thickening since the late Miocene, structural and stratigraphic evidence point to pre-late Miocene shortening and surface uplift.

[65] We suggest that once thick crust built up in the Turkish-Iranian plateau and the interior of the Greater Caucasus, convergence took place more easily by crustal shortening in less elevated regions with initially thinner crust, such as the Zagros Simple Folded Zone, South Caspian region, Kopet Dagh and the foothills of the Greater Caucasus (Figure 7). There are similarities with the late Cenozoic behavior of the Tibetan plateau [*England and Houseman*, 1988; *Molnar et al.*, 1993]; it is easier to absorb continental shortening in regions of thin crust and low elevations, than areas that have undergone shortening and surface uplift and consequently have increased buoyancy forces that resist further shortening. Like the Puna-Altiplano plateau of the Andes [*Sobel et al.*, 2003], internal drainage and ponding of sediment within the basins of the Turkish-Iranian plateau act to increase the gravitational potential energy of the region [*Willett and Beaumont*, 1994]. Westward transport of Turkey between the North and East Anatolian faults has also accommodated part of the plate convergence since ~3–5 Ma. Inactive strike-slip faults in Anatolia may have performed this role before activity began on the present structures [*Westaway and Arger*, 2001].

[66] Delamination of part of the mantle lithosphere has been suggested as the cause of the magmatism and a contributor to the Turkish-Iranian plateau's present elevation [*Pearce et al.*, 1990]. In support of this idea, the plateau has a seismic shear wave low velocity zone and a long wavelength gravity high (50 mgals at a wavelength of ~800 km) [*Hearn and Ni*, 1994; *Maggi et al.*, 2002], both of which indicate an increase in mantle temperature beneath at least part of the plateau. However, magmatism dates back to at least 11 Ma [*Keskin et al.*, 1998], and pre-dates at least some shortening [*National Iranian Oil Company*, 1977b], making it unlikely that there was a sudden and regional delamination event.

[67] In some of the actively deforming areas there is a good match between the finite deformation, and the value reached by extrapolating the active slip rate by the time over which deformation is known to have occurred. Specific examples are the East Anatolian Fault, the Kopet Dagh and the South Caspian Basin (Table 1). Other areas are inconclusive, because either the timing of deformation or the total slip is not known in enough detail. The Alborz, Zagros and eastern Iran are in this category.

[68] The short- and long-term slip rates on the North Anatolian Fault have previously been suggested to match [*McClusky et al.*, 2000; *Bozkurt*, 2001], although the GPS-derived rate for active slip (24 ± 1 mm yr^{-1}) extrapolates to 120 ± 5 km over 5 million years, which is greater than the consensus value for the finite slip of 80–85 km [*Barka et al.*, 2000]. More work is needed to see if this mismatch is because the active slip rate is indeed faster than the long-term average value, or because there are errors in the estimates for the finite slip, timing of fault initiation, or both. It is notable that a late Pliocene age for fault initiation [*Ünay et al.*, 2001] would produce a closer match between short-term and average long-term behavior (24 mm yr^{-1} over ~3 million years equals ~72 km).

[69] In summary, available data suggest that the present deformation rates on major active fault systems would account for the finite strain in these areas in ~3–7 million years, i.e., no further back than the late Miocene. Either the modern slip rates are significantly faster than the long-term average rates – for which there is no evidence, or pre-late Miocene strain in the collision took place in other areas or in other ways. The most likely areas are the Turkish-Iranian plateau and, possibly, the interior of the Greater Caucasus, where there is little sign of active shortening in regions of elevated and thickened crust, but evidence for shortening and uplift before the late Miocene. The timing, style and duration of the changeover to the actively shortening areas need further study.

[70] **Acknowledgments.** This work arises out of the longstanding collaboration between the CASP, the Department of Earth Sciences at the University of Cambridge, the Geological Survey of Iran and the Geology Institute of the Azerbaijan Academy of Sciences. The industry sponsors of CASP's research are thanked for their support. Eric Blanc, Zvi Garfunkel, Mohammad Ghassemi, Arif Ismail-Zadeh, Steve Jones, Nadine McQuarrie, Peter Molnar, Rob Reilinger, Amir Sagi, Mike Simmons, Morteza Talebian and Steve Vincent gave useful insights. Reviews by Anke Friedrich, David Evans and an anonymous referee are gratefully acknowledged. Cambridge University Department of Earth Sciences contribution 7706.

References

Alavi, M. (1994), Tectonics of the Zagros orogenic belt of Iran: new data and interpretations, *Tectonophysics*, *239*, 211–238.

Aliev, A. K. (1960), *Geology and Hydrocarbons of the Kura-Araks Region*, 361 pp., Azerbaijan State Publ. of Hydrocarbon Lit., Baku.

Ali-Zade, A. A., S. G. Salaev, and A. I. Aliev (1985), *Scientific Assessment of Hydrocarbon Prospects in Azerbaijan and the South Caspian and the Direction of Exploration Work*, 250 pp., Elm, Baku.

Allen, M. B., S. Jones, A. Ismail-Zadeh, M. D. Simmons, and L. Anderson (2002), Onset of subduction as the cause of rapid Pliocene-Quaternary subsidence in the South Caspian Basin, *Geology*, *30*, 775–778.

Allen, M. B., M. R. Ghassemi, M. Shahrabi, and M. Qorashi (2003a), Accommodation of late Cenozoic oblique shortening in the Alborz range, northern Iran, *J. Struct. Geol.*, *25*, 659–672.

Allen, M. B., S. J. Vincent, G. I. Alsop, A. Ismail-zadeh, and R. Flecker (2003b), Late Cenozoic deformation in the South Caspian region: Effects of a rigid basement block within a collision zone, *Tectonophysics*, *366*, 223–239.

Annells, R. N., R. S. Arthurton, R. A. Bazley, and R. G. Davies (1975), *Explanatory Text of the Qazvin and Rasht Quadrangles Map*, 94 pp., Geol. Surv. of Iran, Tehran.

Armijo, R., B. Meyer, A. Hubert, and A. Barka (1999), Westward propagation of the North Anatolian fault into the northern Aegean: Timing and kinematics, *Geology*, *27*, 267–270.

Axen, G. J., P. S. Lam, M. Grove, D. F. Stockli, and J. Hassanzadeh (2001), Exhumation of the west-central Alborz Mountains, Iran, Caspian subsidence, and collision-related tectonics, *Geology*, *29*, 559–562.

Azizbekov, S. A. (1972), *Geology of the USSR: Azerbaijan SSR*, 433 pp., Nauka, Moscow.

Banks, C., A. Robinson, and M. Williams (1997), Structure and regional tectonics of the Achara-Trialet fold belt and the adjacent Rioni and Kartli foreland basins, republic of Georgia, in *Regional and Petroleum Geology of the Black Sea and Surrounding Region*, edited by A. Robinson, *AAPG Mem.*, *68*, 331–346.

Barka, A. (1992), The North Anatolian fault zone, *Ann. Tectonicae*, *6*, 164–195.

Barka, A. A., and P. L. Hancock (1984), Neotectonic deformation patterns in the convex-northwards arc of the North Anatolian fault, in *The Geological*

Evolution of the Eastern Mediterranean, edited by J. E. Dixon and A. H. F. Robertson, *Geol. Soc. Spec. Publ.*, *17*, 763–773.

Barka, A., H. S. Akyüz, H. A. Cohen, and F. Watchorn (2000), Tectonic evolution of the Niksar and Tasova-Erbaa pull-apart basins, North Anatolian Fault Zone: Their significance for the motion of the Anatolian block, *Tectonophysics*, *322*, 243–264.

Berberian, F., I. D. Muir, R. J. Pankhurst, and M. Berberian (1982), Late Cretaceous and early Miocene Andean-type plutonic activity in northern Makran and Central Iran, *J. Geol. Soc. London*, *139*, 605–614.

Berberian, M. (1997), Seismic sources of the Transcaucasian historical earthquakes, in *Historical and prehistorical earthquakes in the Caucasus*, edited by D. Giardini and S. Balassanian, pp. 233–311, Kluwer Acad., Norwell, Mass.

Berberian, M., and G. C. P. King (1981), Towards a paleogeography and tectonic evolution of Iran, *Can. J. Earth Sci.*, *18*, 210–265.

Blanc, E. J.-P., M. B. Allen, S. Inger, and H. Hassani (2003), Structural styles in the Zagros Simple Folded Zone, Iran, *J. Geol. Soc. London*, *160*, 401–412.

Bozkurt, E. (2001), Neotectonics of Turkey—A synthesis, *Geodin. Acta*, *14*, 3–30.

Brunet, M. F., M. V. Korotaev, A. V. Ershov, and A. M. Nikishin (2003), The South Caspian Basin: A review of its evolution from subsidence modelling, *Sediment. Geol.*, *156*, 119–146.

Colman-Sadd, S. P. (1978), Fold development in Zagros simple folded belt, SW Iran, *AAPG Bull.*, *62*, 984–1003.

Coskun, B. (2000), North Anatolian Fault-Saros Gulf relationships and their relevance to hydrocarbon exploration, northern Aegean Sea, Turkey, *Mar. Pet. Geol.*, *17*, 751–772.

DeMets, C., R. G. Gordon, D. F. Argus, and S. Stein (1990), Current plate motions, *Geophys. J. Int.*, *101*, 425–478.

DeMets, C., R. G. Gordon, D. F. Argus, and S. Stein (1994), Effects of recent revisions to the geomagnetic time scale on estimates of current plate motions, *Geophys. Res. Lett.*, *21*, 2191–2194.

Devlin, W., J. Cogswell, G. Gaskins, G. Isaksen, D. Pitcher, D. Puls, K. Stanley, and G. Wall (1999), South Caspian Basin: Young, cool, and full of promise, *GSA Today*, *9*(7), 1–9.

Dewey, J. F., M. R. Hempton, W. S. F. Kidd, F. Saroglu, and A. M. C. Sengor (1986), Shortening of continental lithosphere: The neotectonics of eastern Anatolia, a young collision zone, in *Collision Tectonics*, edited by M. P. Coward and A. C. Ries, *Geol. Soc. Spec. Publ.*, *19*, 3–36.

Dewey, J. F., M. L. Helman, E. Turco, D. H. W. Hutton and S. D. Knott (1989), Kinematics of the western Mediterranean, in *Alpine Tectonics*, edited by M. P. Coward, D. Dietrich, and R. G. Park, *Geol. Soc. Spec. Publ.*, *45*, 265–283.

Dotduyev, S. I. (1986), The nappe structure of the Greater Caucasus, *Geotectonics*, *20*, 420–430.

Elmore, R. D., and W. R. Farrand (1981), Asphalt-bearing sediment in synorogenic Miocene-Pliocene molasse, Zagros mountains, Iran, *AAPG Bull.*, *65*, 1160–1165.

Engdahl, E. R., R. van der Hilst, and R. Buland (1998), Global teleseismic earthquake relocation with improved travel times and procedures for depth determination, *Seismol. Soc. Am. Bull.*, *88*, 722–743.

England, P. C., and G. A. Houseman (1988), The mechanics of the Tibetan plateau, *Philos. Trans. R. Soc. London*, *326*, 301–319.

Ershov, A. V., M. F. Brunet, A. M. Nikishin, S. N. Bolotov, B. P. Nazarevich, and M. V. Korotaev (2003), Northern Caucasus basin: Thermal history and synthesis of subsidence models, *Sediment. Geol.*, *156*, 95–118.

Eyal, M., Y. Eyal, Y. Bartov, and G. Steinitz (1981), The tectonic development of the western margin of the Gulf of Elat, Aqaba, rift, *Tectonophysics*, *80*, 39–66.

Falcon, N. (1974), Southern Iran: Zagros mountains, in *Mesozoic-Cenozoic Orogenic belts: Data for Orogenic Studies*, edited by A. Spencer, *Geol. Soc. Spec. Publ.*, *4*, 199–211.

Freund, R. (1970), Rotation of strike-slip faults in Sistan, southeast Iran, *J. Geol.*, *78*, 188–200.

Garfunkel, Z. (1981), Internal structure of the Dead Sea leaky transform (rift) in relation to plate kinematics, *Tectonophysics*, *80*, 81–108.

Gazis, C. A., M. Lanphere, H. P. Taylor, and A. Gurbanov (1995), Ar^{40}/Ar^{39} and O^{18}/O^{16} studies of the Chegem ash-flow caldera and the Eldjurta granite: Cooling of two late Pliocene igneous bodies in the Greater Caucasus mountains, Russia, *Earth Planet. Sci. Lett.*, *134*, 377–391.

Geological Survey of Iran (1975), Geological map of Maku, scale 1:250,000, Geol. Survey of Iran, Tehran.

Geological Survey of Iran (1978), Geological map of Mianeh, scale 1:250,000, Geol. Survey of Iran, Tehran.

Geological Survey of Iran (1987), Geological map of Tehran, scale 1:250,000, Geol. Survey of Iran, Tehran.

Geological Survey of Iran (1994), Geological map of Moghan, scale 1:250,000, Geol. Survey of Iran, Tehran.

Ginat, H., Y. Enzel, and Y. Avni (1998), Translocated Plio-Pleistocene drainage systems along the Arava fault of the Dead Sea transform, *Tectonophysics*, *284*, 151–160.

Hearn, T. N., and J. F. Ni (1994), Pn velocities beneath continental collision zones: The Turkish-Iranian Plateau, *Geophys. J. Int.*, *117*, 273–283.

Hempton, M. R. (1985), Structure and deformation history of the Bitlis suture near Lake Hazar, southeastern Turkey, *Geol. Soc. Am. Bull.*, *96*, 233–243.

Hempton, M. R. (1987), Constraints on Arabian plate motion and extensional history of the Red Sea, *Tectonics*, *6*, 687–705.

Jackson, J. (1992), Partitioning of strike-slip and convergent motion between Eurasia and Arabia in eastern Turkey and the Caucasus, *J. Geophys. Res.*, *97*, 12,471–12,479.

Jackson, J. A., and D. P. McKenzie (1984), Active tectonics of the Alpine-Himalayan belt between western Turkey and Pakistan, *Geophys. J. R. Astron. Soc.*, *77*, 185–264.

Jackson, J., and D. McKenzie (1988), The relationship between plate motion and seismic moment tensors, and the rates of active deformation in the Mediterranean and Middle East, *Geophys. J. R. Astron. Soc.*, *93*, 45–73.

Jackson, J., A. J. Haines, and W. E. Holt (1995), The accommodation of Arabia-Eurasia plate convergence in Iran, *J. Geophys. Res.*, *100*, 15,205–15,209.

Jackson, J., K. Priestley, M. Allen, and M. Berberian (2002), Active tectonics of the South Caspian Basin, *Geophys. J. Int.*, *148*, 214–245.

Jaffey, N., and A. H. F. Robertson (2001), New sedimentological and structural data from the Ecemis Fault Zone, southern Turkey: Implications for its timing and offset and the Cenozoic tectonic escape of Anatolia, *J. Geol. Soc. London*, *158*, 367–378.

James, G. A., and J. G. Wynd (1965), Stratigraphic nomenclature of the Iranian oil consortium agreement area, *AAPG Bull.*, *49*, 2182–2245.

Keskin, M., J. A. Pearce, and J. G. Mitchell (1998), Volcano-stratigraphy and geochemistry of collision-related volcanism on the Erzurum-Kars Plateau, northeastern Turkey, *J. Volcanol. Geotherm. Res.*, *85*, 355–404.

Klinger, Y., J. P. Avouac, N. Abou Karaki, L. Dorbath, D. Bourles, and J. L. Reyss (2000), Slip rate on the Dead Sea transform fault in northern Araba valley (Jordan), *Geophys. J. Int.*, *142*, 755–768.

Koçyigit, A., A. Yılmaz, S. Adamia, and S. Kuloshvili (2001), Neotectonics of East Anatolian Plateau (Turkey) and Lesser Caucasus: Implication for transition from thrusting to strike-slip faulting, *Geodin. Acta*, *14*, 177–195.

Lyberis, N., and G. Manby (1999), Oblique to orthogonal convergence across the Turan Block in the Post-Miocene, *AAPG Bull.*, *83*, 1135–1160.

Lyberis, N., T. Yürür, J. Chorowicz, E. Kasapoglu, and N. Gündogdu (1992), The East Anatolian Fault: An oblique collisional belt, *Tectonophysics*, *204*, 1–15.

Maggi, A., J. A. Jackson, K. Priestley, and C. Baker (2000), A re-assessment of focal depth distributions in southern Iran, the Tien Shan and northern India: Do earthquakes really occur in the continental mantle?, *Geophys. J. Int.*, *143*, 629–661.

Maggi, A., K. Priestley, and D. McKenzie (2002), Seismic structure of the Middle East, *Eos Trans. AGU*, *83*(47), Fall Meet. Suppl., Abstract S51B-1041.

Mangino, S., and K. Priestley (1998), The crustal structure of the southern Caspian region, *Geophys. J. Int.*, *133*, 630–648.

Manspeizer, W. (1985), The Dead Sea Rift: Impact of climate and tectonism on Pleistocene and Holocene sedimentation, in *Strike-Slip Deformation, Basin Formation and Sedimentation*, edited by K. Biddle and N. Christie-Blick, *Spec. Publ. SEPM Soc. Sediment. Geol.*, *37*, 143–158.

McClusky, S., et al. (2000), Global Positioning System constraints on plate kinematics and dynamics in the eastern Mediterranean and Caucasus, *J. Geophys. Res.*, *105*, 5695–5719.

McClusky, S., R. Reilinger, S. Mahmoud, D. Ben Sari, and A. Tealeb (2003), GPS constraints on Africa (Nubia) and Arabia plate motions, *Geophys. J. Int.*, *155*, 126–138.

McKenzie, D. P. (1972), Active tectonics of the Mediterranean region, *Geophys. J. R. Astron. Soc.*, *30*, 109–185.

McQuarrie, N. (2004), Crustal-scale geometry of the Zagros fold-thrust belt, Iran, *J. Struct. Geol.*, *26*, 519–535.

McQuarrie, N., J. M. Stock, C. Verdel, and B. Wernicke (2003), Cenozoic evolution of Neotethys and implications for the causes of plate motions, *Geophys. Res. Lett.*, *30*(20), 2036, doi:10.1029/2003GL017992.

Mikhailov, V. O., L. V. Panina, R. Polino, N. V. Koronovsky, E. A. Kiseleva, N. V. Klavdieva, and E. I. Smolyaninova (1999), Evolution of the North Caucasus foredeep: Constraints based on the analysis of subsidence curves, *Tectonophysics*, *307*, 361–379.

Molnar, P., P. England, and J. Martinod (1993), Mantle dynamics, uplift of the Tibetan plateau and the Indian monsoon, *Rev. Geophys.*, *31*, 357–396.

Morton, A., M. Allen, M. Simmons, F. Spathopoulos, J. Still, D. Hinds, A. Ismail-Zadeh, and S. B. Kroonenberg (2003), Provenance patterns in a neotectonic basin: Pliocene and Quaternary sediment supply to the South Caspian, *Basin Res.*, *15*, 321–337.

Nalivkin, D. V. (1983), Geological map of the USSR and adjacent water-covered areas, scale 1:2,500,000, Minist. of Geol. of the USSR, Moscow.

National Iranian Oil Company (1975), Geological map of Iran, sheet 4 south-west Iran, scale 1:1,000,000, Natl. Iranian Oil Co., Tehran.

National Iranian Oil Company (1977a), Geological map of Iran, sheet 5 south-central Iran, scale 1:1,000,000, Natl. Iranian Oil Co., Tehran.

National Iranian Oil Company (1977b), Geological cross-sections north-west Iran, Natl. Iranian Oil Co., Tehran.

National Iranian Oil Company (1978), Geological map of Iran, sheet 1 north-west Iran, scale 1:1,000,000, Natl. Iranian Oil Co., Tehran.

Neprochnov, Y. P. (1968), Structure of the Earth's crust of epi-continental seas: Caspian, Black and Mediterranean, *Can. J. Earth Sci.*, *5*, 1037–1043.

Niemi, T. M., H. W. Zhang, M. Atallah, and J. B. J. Harrison (2001), Late Pleistocene and Holocene slip rate of the Northern Wadi Araba fault, Dead Sea Transform, Jordan, *J. Seismol.*, *5*, 449–474.

O'B Perry, J. T., and A. Setudehnia (1966), Masjed-e-Suleyman, scale 1:100,000, Iranian Oil Oper. Co., Tehran.

Pearce, J. A., J. F. Bender, S. E. Delong, W. S. F. Kidd, P. J. Low, Y. Güner, F. Şaroglu, Y. Yılmaz, S. Moorbath, and J. G. Mitchell (1990), Genesis of collision volcanism in eastern Anatolia, Turkey, *J. Volcanol. Geotherm. Res.*, *44*, 189–229.

Pe'eri, S., S. Wdowinski, A. Shtibelman, N. Bechor, Y. Bock, R. Nikolaidis, and M. van Domselaar (2002), Current plate motion across the Dead Sea Fault from three years of continuous GPS monitoring, *Geophys. Res. Lett.*, *29*(14), 1697, doi:10.1029/2001GL013879.

Philip, H., A. Cisternas, A. Gvishiani, and A. Gorshkov (1989), The Caucasus: An actual example of the initial stages of a continental collision, *Tectonophysics*, *161*, 1–21.

Priestley, K., C. Baker, and J. Jackson (1994), Implications of earthquake focal mechanism data for the active tectonics of the South Caspian Basin and surrounding regions, *Geophys. J. Int.*, *118*, 111–141.

Quennell, A. M. (1958), The structure and evolution of the Dead Sea rift, *Q. J. Geol. Soc. London*, *64*, 1–24.

Quennell, A. M. (1984), The Western Arabia rift system, in *The Geological Evolution of the Eastern Mediterranean*, edited by J. E. Dixon and A. H. F. Robertson, *Geol. Soc. Spec. Publ.*, *17*, 775–788.

Reilinger, R. E., S. C. McClusky, B. J. Souter, M. W. Hamburger, M. T. Prilepin, A. Mishin, T. Guseva, and S. Baslassanian (1997), Preliminary estimates of plate convergence in the Caucasus collision zone from global positioning system measurements, *Geophys. Res. Lett.*, *24*, 1815–1818.

Robertson, A. H. F. (2000), Mesozoic-Tertiary tectonic-sedimentary evolution of a south Tethyan oceanic basin and its margins in southern Turkey, in *Tectonics and Magmatism in Turkey and the Surrounding Area*, edited by E. Bozkurt, J. A. Winchester, and J. D. A. Piper, *Geol. Soc. Spec. Publ.*, *173*, 97–138.

Rogozhin, Y. E., and V. N. Sholpo (1988), Inhomogeneity of the zone of similar folding in the Greater Caucasus, *Geotectonics*, *22*, 446–456.

Ruppel, C., and M. McNutt (1990), Regional compensation of the Greater Caucasus mountains based on an analysis of Bouguer gravity data, *Earth Planet. Sci. Lett.*, *98*, 360–379.

Sandvol, E., D. Seber, A. Calvert, and M. Barazangi (1998), Grid search modeling of receiver functions: Implications for crustal structure in the Middle East and North Africa, *J. Geophys. Res.*, *103*, 26,899–26,917.

Şaroglu, F., Ö. Emre, and Ý. Kuşçu (1992), The East Anatolian Fault of Turkey, *Ann. Tectonicae*, *6*, 125–199.

Seber, D., E. Sandvol, C. Sandvol, C. Brindisi, and M. Barazangi (2001), Crustal model for the Middle East and North Africa region: Implications for the isostatic compensation mechanism, *Geophys. J. Int.*, *147*, 630–638.

Sella, G. F., T. H. Dixon, and A. Mao (2002), REVEL: A model for Recent plate velocities from space geodesy, *J. Geophys. Res.*, *107*(B4), 2081, doi:10.1029/2000JB000033.

Şengör, A. M. C. (1990), A new model for the late Palaeozoic-Mesozoic tectonic evolution of Iran and implications for Oman, in *The Geology and Tectonics of the Oman Region*, edited by A. H. F. Robertson, M. P. Searle, and A. C. Ries, *Geol. Soc. Spec. Publ.*, *49*, 797–831.

Şengör, A. M. C., and W. S. F. Kidd (1979), Post-collisional tectonics of the Turkish-Iranian plateau and a comparison with Tibet, *Tectonophysics*, *55*, 361–376.

Şengör, A., N. Görür, and F. Şaroglu (1985), Strike-slip faulting and related basin formation in zones of tectonic escape: Turkey as a case study, in *Strike-Slip Deformation, Basin Formation and Sedimentation*, edited by K. Biddle and N. Christie-Blick, *Spec. Publ. SEPM Soc. Sediment. Geol.*, SEPM, *37*, 227–264.

Seymen, İ. (1975), Tectonic characteristics of the North Anatolian Fault zone in the Kelkit Valley segment, Ph.D., 198 pp., Istanbul Teknik Univ., Maden Fakultesi, Yayinlari, Istanbul, Turkey.

Sneh, A. (1996), The Dead Sea Rift: Lateral displacement and downfaulting phases, *Tectonophysics*, *263*, 277–292.

Snyder, D. B., and M. Barazangi (1986), Deep crustal structure and flexure of the Arabian plate beneath the Zagros collisional mountain belt as inferred from gravity observations, *Tectonics*, *5*, 361–373.

Sobel, E. R., G. E. Hilley, and M. R. Strecker (2003), Formation of internally drained contractional basins by aridity-limited bedrock incision, *J. Geophys. Res.*, *108*(B7), 2344, doi:10.1029/2002JB001883.

Sobornov, K. O. (1994), Structure and petroleum potential of the Dagestan thrust belt, northeastern Caucasus, Russia, *Bull. Can. Pet. Geol.*, *42*, 352–364.

Stöcklin, J. (1971), *Stratigraphic Lexicon of Iran Part 1: Central, North and East Iran*, 338 pp., Geol. Surv. of Iran, Tehran.

Stoneley, R. (1981), The geology of the Kuh-e Dalneshin area of southern Iran and its bearing on the evolution of southern Tethys, *J. Geol. Soc. London*, *138*, 509–526.

Talebian, M., and J. A. Jackson (2002), Offset on the Main Recent Fault of NW Iran and implications for the late Cenozoic tectonics of the Arabia-Eurasia collision zone, *Geophys. J. Int.*, *150*, 422–439.

Talebian, M., and J. Jackson (2004), A reappraisal of earthquake focal mechanisms and active shortening in the Zagros mountains of Iran, *Geophys. J. Int.*, in press.

Tatar, M. (2001), Etude Seismotectonique de deux zones de collision continentale: Le Zagros Central et l'Alborz (Iran), Ph.D. thesis, 204 pp., Univ. de Joseph Fourier, Grenoble, France.

Tatar, M., D. Hatzfeld, J. Martinod, A. Walpersdorf, M. Ghafori-Ashtiany, and J. Chery (2002), The present-day deformation of the central Zagros from GPS measurements, *Geophys. Res. Lett.*, *29*(19), 1927, doi:10.1029/2002GL015427.

Taymaz, T., J. A. Jackson, and D. McKenzie (1991), Active tectonics of the north and central Aegean Sea, *Geophys. J. Int.*, *106*, 403–490.

Tirrul, R., I. R. Bell, R. J. Griffis, and V. E. Camp (1983), The Sistan suture zone of eastern Iran, *Geol. Soc. Am. Bull.*, *94*, 134–150.

Toloczyki, M., P. Trunit, and A. Voges (1994), Geological map, sheet F5, Tbilisi, scale 1:1,500,000, Int. Geol. Congress, Hannover, Germany.

Triep, E. G., G. A. Abers, A. L. Lerner-Lam, V. Mihatkin, N. Zakharchenko, and O. Starovoit (1995), Active thrust front of the Greater Caucasus: The April 29, 1991 Racha earthquake sequence and its tectonic implications, *J. Geophys. Res.*, *100*, 4011–4034.

Trifonov, V. G. (1978), Late Quaternary tectonic movements of western and central Asia, *Geol. Soc. Am. Bull.*, *89*, 1059–1072.

Tüysüz, O., A. Barka, and E. Yigitbaş (1998), Geology of the Saros graben and its implications for the evolution of the North Anatolian fault in the Ganos-Saros region, northwestern Turkey, *Tectonophysics*, *293*, 105–126.

Ünay, E., Ö. Emre, T. Erkal, and M. Keçer (2001), The rodent fauna from the Adapazarı pull-apart basin (NW Anatolia): Its bearings on the age of the North Anatolian fault, *Geodin. Acta*, *14*, 169–175.

Vincent, S. J., M. B. Allen, A. Ismail-zadeh, and R. Flecker (2002), The Paleogene evolution and sedimentary fill of the South Caspian Basin: Insights from the Talysh of southern Azerbaijan, paper presented at Geological Society of London meeting on Petroleum Geology of the Caspian Basins, London, UK.

Walker, R., and J. Jackson (2002), Offset and evolution of the Gowk fault, S. E. Iran: A major intra-continental strike-slip system, *J. Struct. Geol.*, *24*, 1677–1698.

Wells, A. J. (1969), The Crush Zone of the Iranian Zagros Mountains, and its implications, *Geol. Mag.*, *106*, 385–394.

Westaway, R. (1994), Present-day kinematics of the Middle East and eastern Mediterranean, *J. Geophys. Res.*, *99*, 12,071–12,090.

Westaway, R., and J. Arger (1996), The Golbasi basin, southeastern Turkey: A complex discontinuity in a major strike-slip fault zone, *J. Geol. Soc. London*, *153*, 729–743.

Westaway, R., and J. Arger (2001), Kinematics of the Malatya-Ovacik fault zone, *Geodin. Acta*, *14*, 103–131.

Willett, S. D., and C. Beaumont (1994), Subduction of Asian lithospheric mantle beneath Tibet inferred from models of continental collision, *Nature*, *369*, 642–645.

Yakubov, A. A., and A. A. Alizade (1971), *Mud Volcanoes of the Azerbaijan SSR*, 258 pp., Publ. House, Acad. of Sci., Azerbaijan SSR, Baku.

Yaltırak, C., M. Sakinç, and F. Y. Oktay (2000), Westward propagation of North Anatolian fault into the northern Aegean: Timing and kinematics: Comment, *Geology*, *28*, 187–188.

Yılmaz, Y. (1993), New evidence and model on the evolution of the southeast Anatolian orogen, *Geol. Soc. Am. Bull.*, *105*, 251–271.

Zor, E., E. Sandvol, C. Gürbüz, N. Türkelli, D. Seber, and M. Barazangi (2003), The crustal structure of the East Anatolian plateau (Turkey) from receiver functions, *Geophys. Res. Lett.*, *30*(24), 8044, doi:10.1029/2003GL018192.

M. Allen, CASP, Department of Earth Sciences, University of Cambridge, Huntingdon Road, Cambridge CB3 ODH, UK. (mark.allen@casp.cam.ac.uk)

J. Jackson and R. Walker, Department of Earth Sciences, Bullard Laboratories, University of Cambridge, Madingley Road, Cambridge CB3 0EZ, UK.

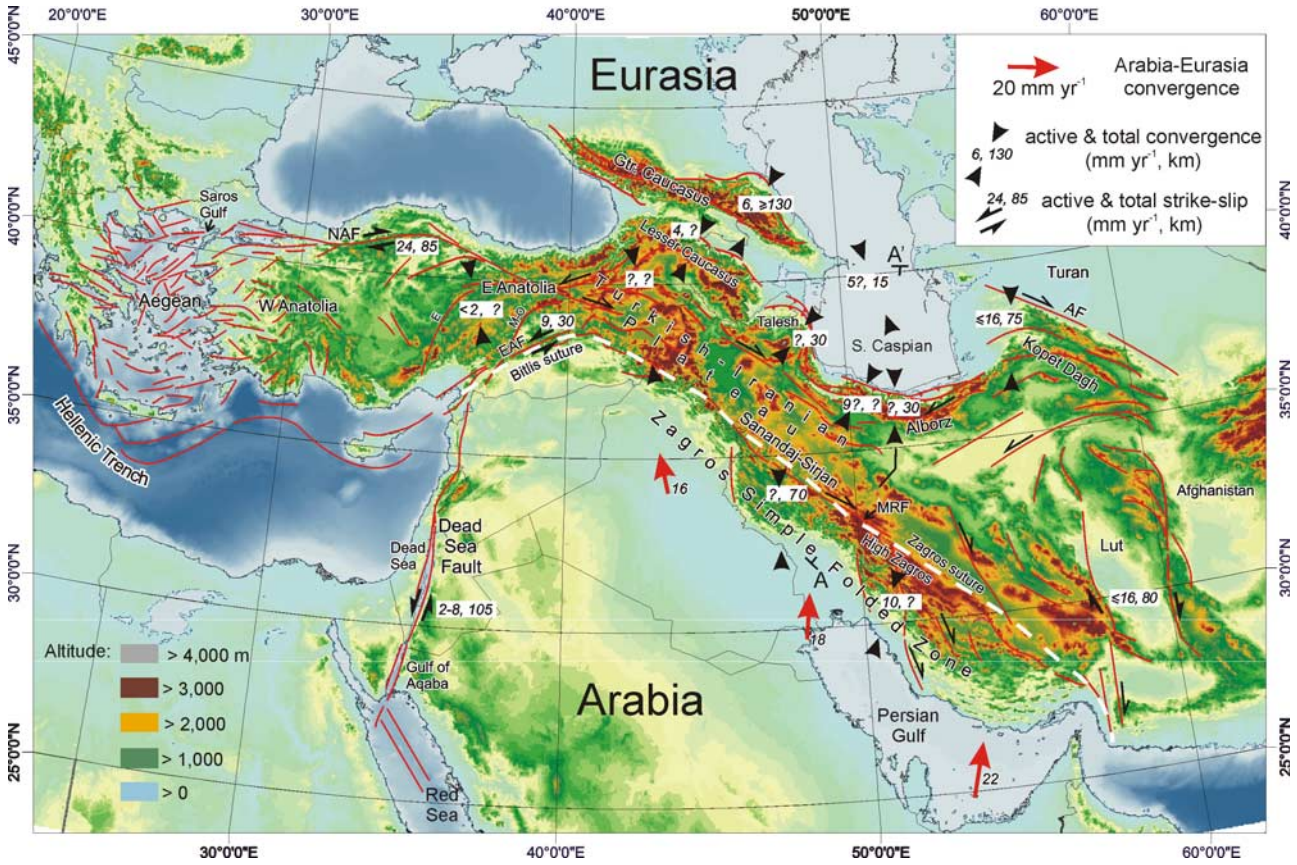

Figure 1. Topography, structure, current deformation rates and finite strain of the Arabia-Eurasia collision. Numbers in italics are present shortening or slip rate in mm yr^{-1}, followed by finite shortening or strike-slip in kilometers; see text for data sources for each area. Abbreviations are as follows: AF, Ashgabat Fault; E, Ecemiş Fault; EAF, East Anatolian Fault; M-O, Malatya-Ovacik Fault; MRF, Main Recent Fault; NAF, North Anatolian Fault. Red lines indicate main active faults, with thrusts marked by barbs. Present Arabia-Eurasia convergence rates from *Sella et al.* [2002]. A-A′ marks the section line of Figure 4.